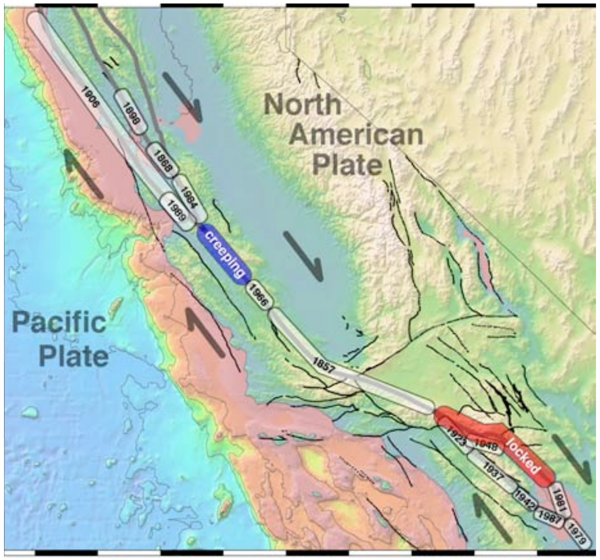

Comparison of Strain Rate Maps

David T. Sandwell
UCERF March 30, 2010

UCERF

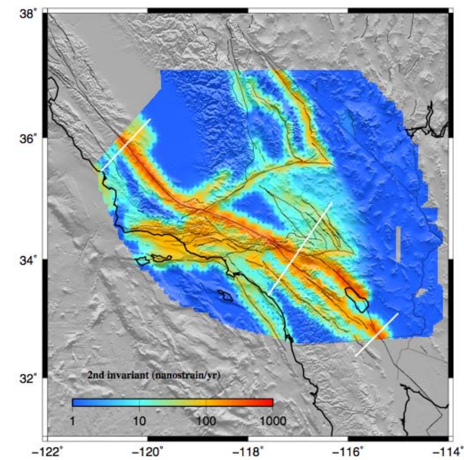

- why strain rate matters
  - elastic stress buildup
  - strain rate effects rheology
  - may help with earthquake forecast?
- comparison of 16 strain rate maps
- secure science
- new data required

Recommendations

(iii) Secure Science and Next Steps for UCERF3

1. How do we assess the accuracy of the strain rate models?

A. We need to perform a synthetic data exercise. We could take an approach like rupture dynamics code validation exercises. We need to start with simple code tests and expand to full tests with locked faults, off fault strain, and errors in data. Approaches should also provide error bounds on strain rate components. Some modest funding is needed to pursue this approach via a focused working group and mini-workshops.

B. We need to show and analyze the already-assembled strain rate data more completely. Such an analysis should show principal components of strain in addition to the second invariant. These data are openly available at ftp://topex.ucsd.edu/pub/sandwell/strain.

Recommendations

(iii) Secure Science and Next Steps for UCERF3

2. *How do we decompose strain rate into elastic and inelastic (e.g., creep)? Three approaches suggest themselves:*

A. We could use the creep data compiled from UCREF2 for a first order correction to the block models.

B. This problem is beyond the scope of what we can do for UCERF3 given that we have less than one seismic cycle worth of GPS data, so it is a topic of future research.

C. We shouldn't worry because the strain is mostly elastic, due to accumulating strain on many small faults.

Recommendations

(iii) Secure Science and Next Steps for UCERF3

1. How do we assess the accuracy of the strain rate models?

A. We need to perform a synthetic data exercise. We could take an approach like rupture dynamics code validation exercises. We need to start with simple code tests and expand to full tests with locked faults, off fault strain, and errors in data. Approaches should also provide error bounds on strain rate components. Some modest funding is needed to pursue this approach via a focused working group and mini-workshops.

B. We need to show and analyze the already-assembled strain rate data more completely. Such an analysis should show principal components of strain in addition to the second invariant. These data are openly available at ftp://topex.ucsd.edu/pub/sandwell/strain.

Recommendations

(iii) Secure Science and Next Steps for UCERF3

1. How do we assess the accuracy of the strain rate models?

A. We need to perform a synthetic data exercise. We could take an approach like rupture dynamics code validation exercises. We need to start with simple code tests and expand to full tests with locked faults, off fault strain, and errors in data. Approaches should also provide error bounds on strain rate components. Some modest funding is needed to pursue this approach via a focused working group and mini-workshops.

B. We need to show and analyze the already-assembled strain rate data more completely. Such an analysis should show principal components of strain in addition to the second invariant. These data are openly available at ftp://topex.ucsd.edu/pub/sandwell/strain.

interseismic model

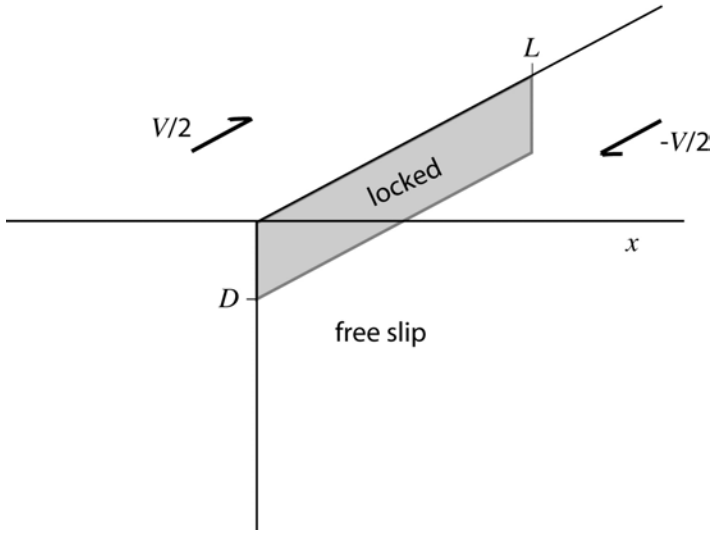

velocity $$v(x) = \frac{V}{\pi} \tan^{-1} \frac{x}{D}$$

strain rate $$\dot{\varepsilon}(x) = \frac{V}{\pi D} \frac{1}{1 + \left(\frac{x}{D}\right)^2}$$ = velocity / depth

moment rate $$\frac{\dot{M}}{L} = \mu V D$$ = velocity X depth

strain rate

$$\dot{\varepsilon} = \frac{v}{\pi d} = \frac{\text{velocity}}{\text{locking depth}}$$

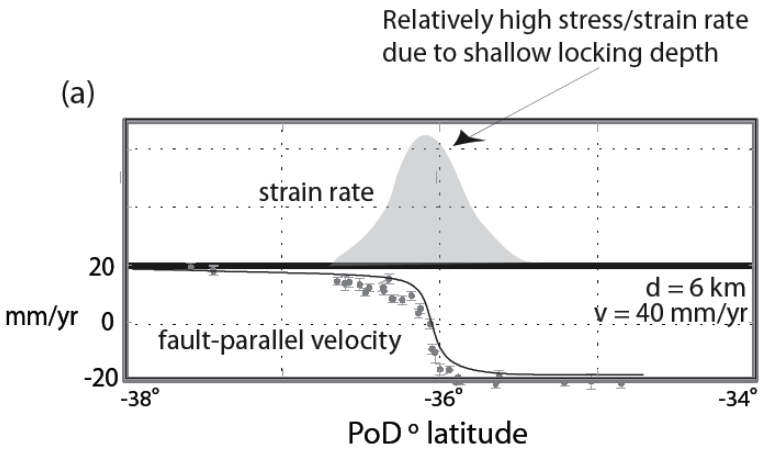

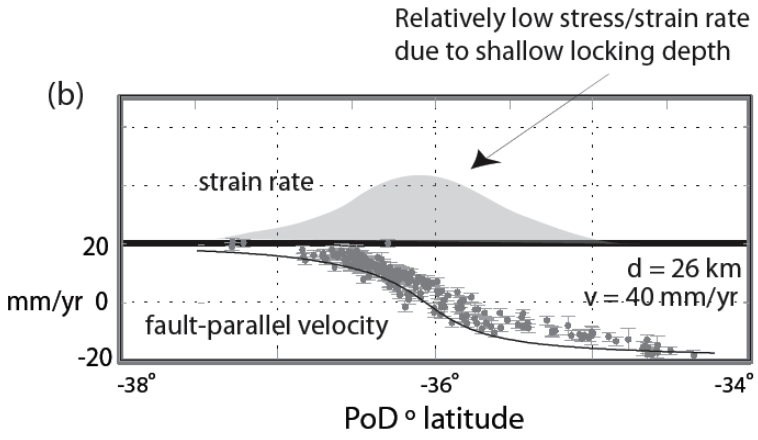

$$\dot{\sigma} = \dot{\tau} - \mu\dot{\sigma}_n$$

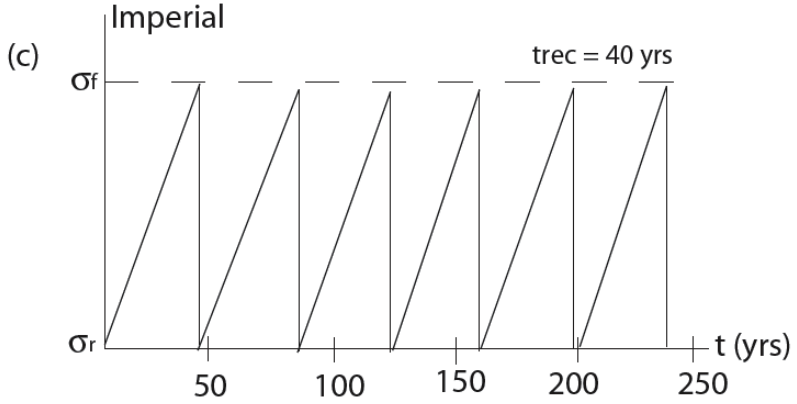

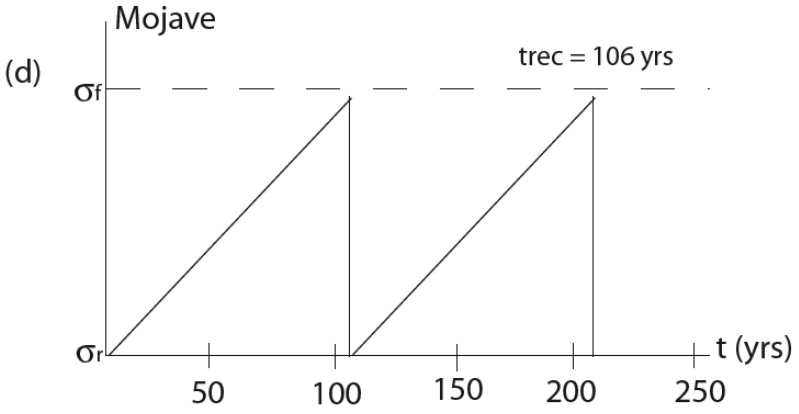

Superstition Hills fault - only the locked zone matters

[Wei et al., 2009]

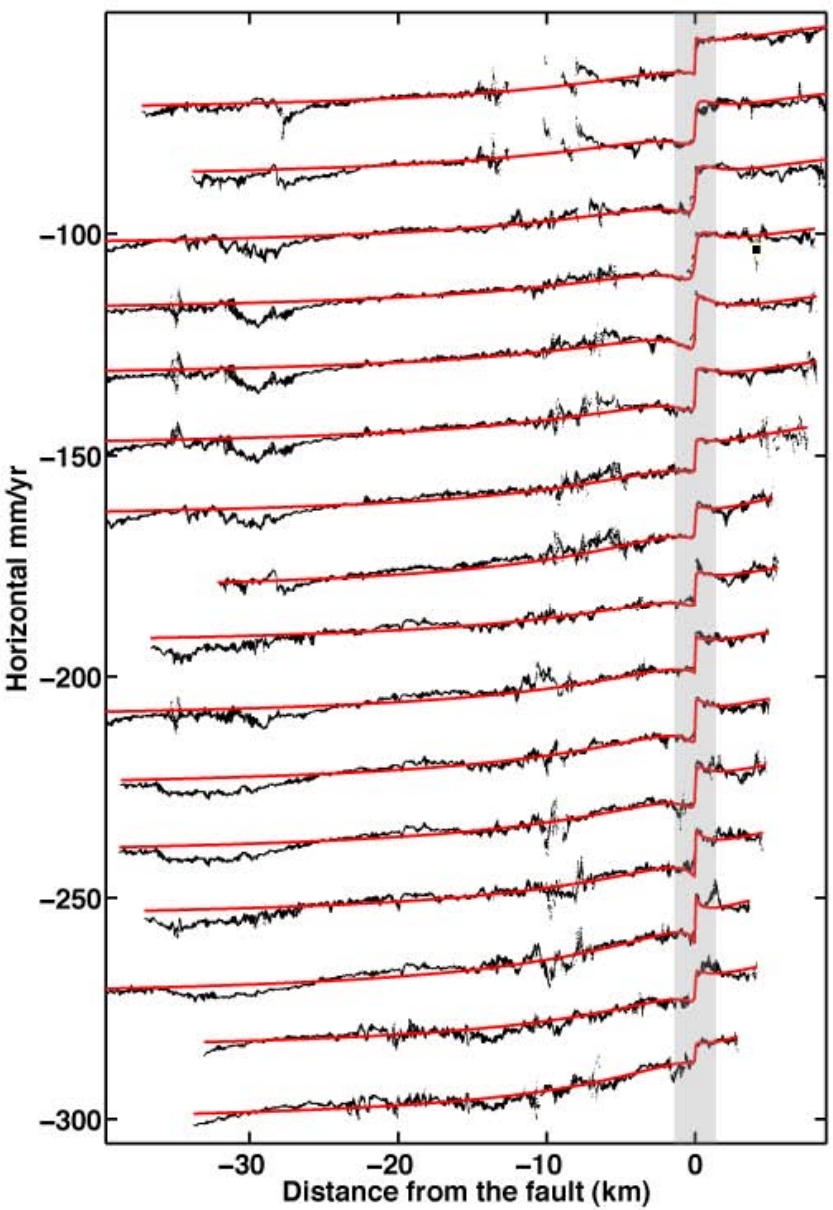

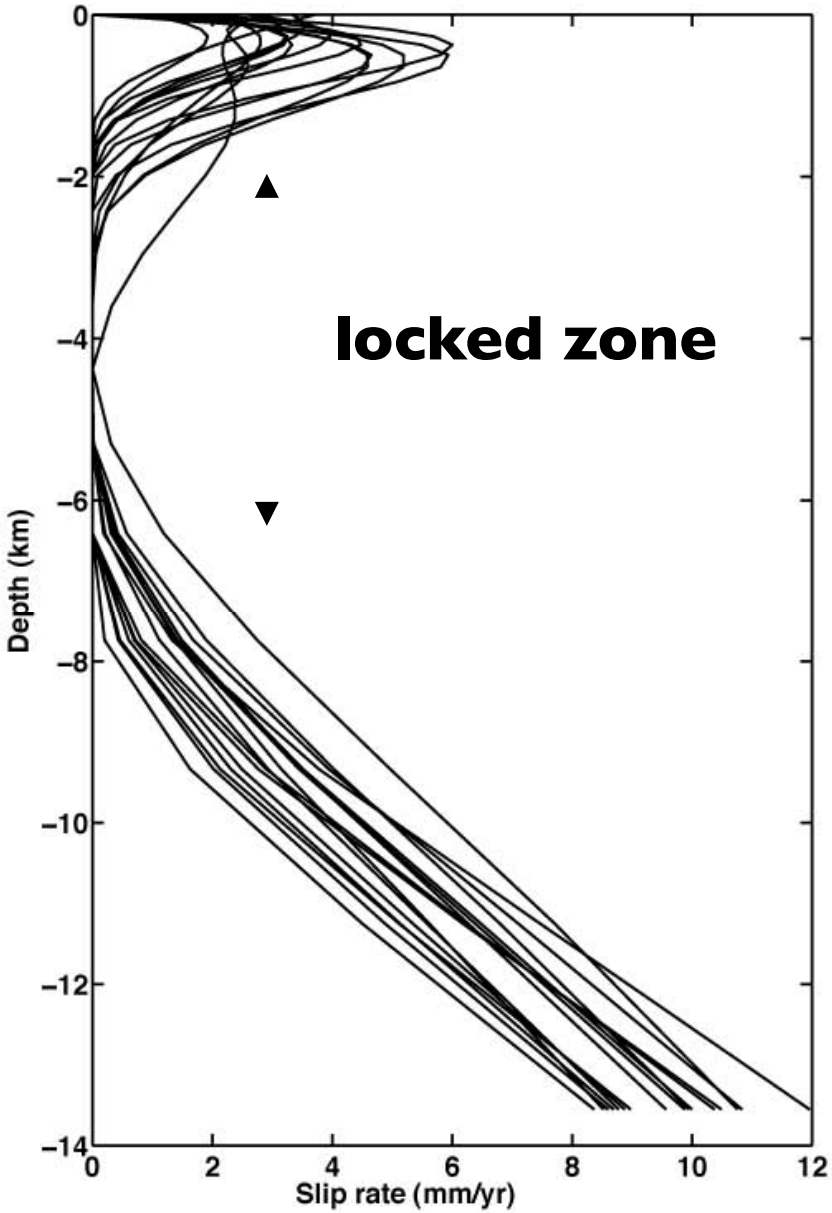

$$\text{UCERF\_strain} = 10^{\text{prob}+3.4}$$

holt

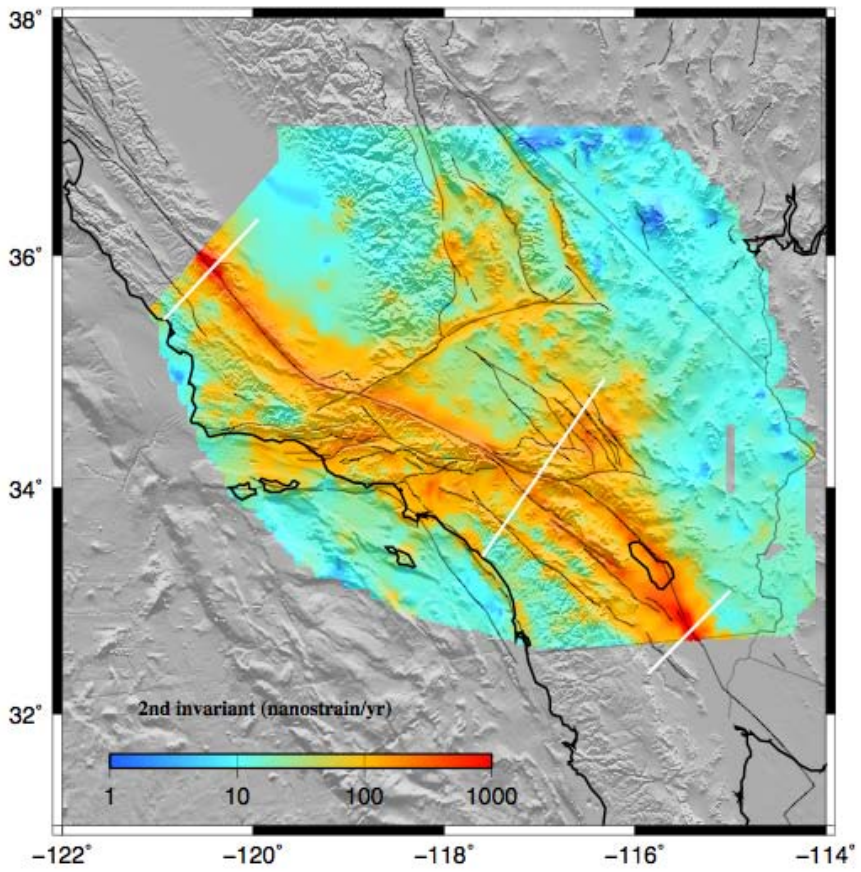

UCERF

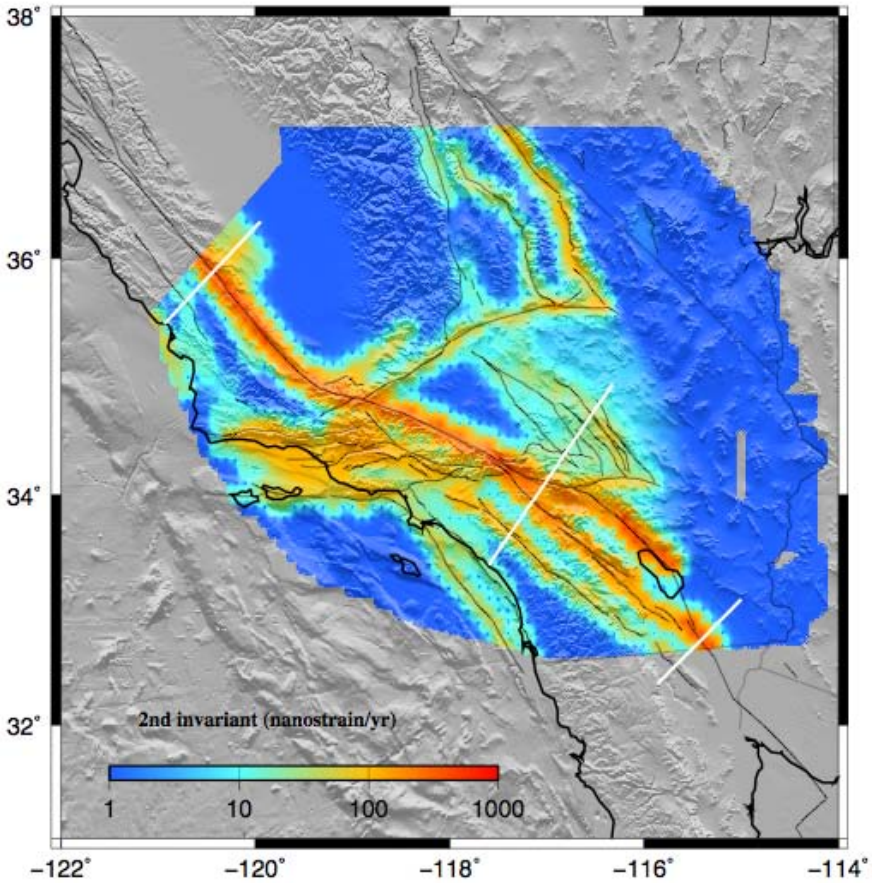

Comparison of Strain-Rate Maps of Western North America

Thorsten Becker, University of Southern California
Peter Bird, University of California at Los Angeles
Jayne Bormann, UNR
Andrew Freed, Purdue University
Brendan Meade, Jack Loveless, Harvard
William Holt, State University of New York, Stony Brook
Ben Hooks, University of Texas at El Paso
Sharon Kedar, Sean Baxter, JPL
Corne Kreemer, University of Nevada
Rob McCaffrey, Rensselaer Polytechnic Institute
Tom Parsons, USGS
Fred Pollitz, USGS Menlo Park
Zeng-Kang Shen, UCLA
Bridget Smith-Konter, University of Texas at El Paso
Carl Tape, Harvard
Yuehua Zeng, USGS, Menlo Park

Velocity to Strain Rate

$v_i\left(x_j^k\right) \pm \sigma_i^k$ - vector velocity at point *k*

$i = 1,2,3 \quad j = 1,2 \quad k = 1 - N$

⇓ 2-D interpolation and/or dislocation model

$v_i\left(x_j\right)$ - surface vector velocity (0.01˚)

⇓ differentiation (GMT grdgradient)

$$\dot{\varepsilon}_{ij} = \frac{1}{2}\left(\frac{\partial v_i}{\partial x_j} + \frac{\partial v_j}{\partial x_i}\right)$$ - 2D strain rate

principal strain rate

$$\dot{\varepsilon}_{1,2} = \frac{\dot{\varepsilon}_{xx} + \dot{\varepsilon}_{yy}}{2} \pm \frac{1}{2}\left\{\left(\dot{\varepsilon}_{xx} - \dot{\varepsilon}_{yy}\right)^2 + 4\dot{\varepsilon}_{xy}^2\right\}^{1/2}$$

dilatation rate + maximum shear rate

second invariant

$$\dot{\varepsilon}_{II} = \left(\dot{\varepsilon}_{xx}^2 + \dot{\varepsilon}_{yy}^2 + 2\dot{\varepsilon}_{xy}^2\right)^{1/2}$$

Different Methods and Assumptions to Overcome Incomplete Spatial Sampling

Four approaches are used, isotropic interpolation, interpolation guided by known faults, interpolation of a rheologically-layered lithosphere, and model fitting using deep dislocations in an elastic layer or half space. This living analysis compares strain rate maps from several groups to establish the common features among the maps, as well as the differences between the maps. These differences reveal the spatial resolution limitations of the GPS array, as well as assumed fault locations and rheological assumptions. Moreover the comparisons promote collaboration among the various groups to establish the best possible strain-rate map.

kedar_baxter

Strain rates calculated with a 30km Gaussian weighting radius per our scheme, generally following the formulation of Feigl et al [1993], i.e., there is no tectonic model involved, just a weighted least squares estimation at every point in the continuum.The attached images of the shear strain field were generated using progressively larger Guassian weighing radius plotted on the same amplitude color scale.

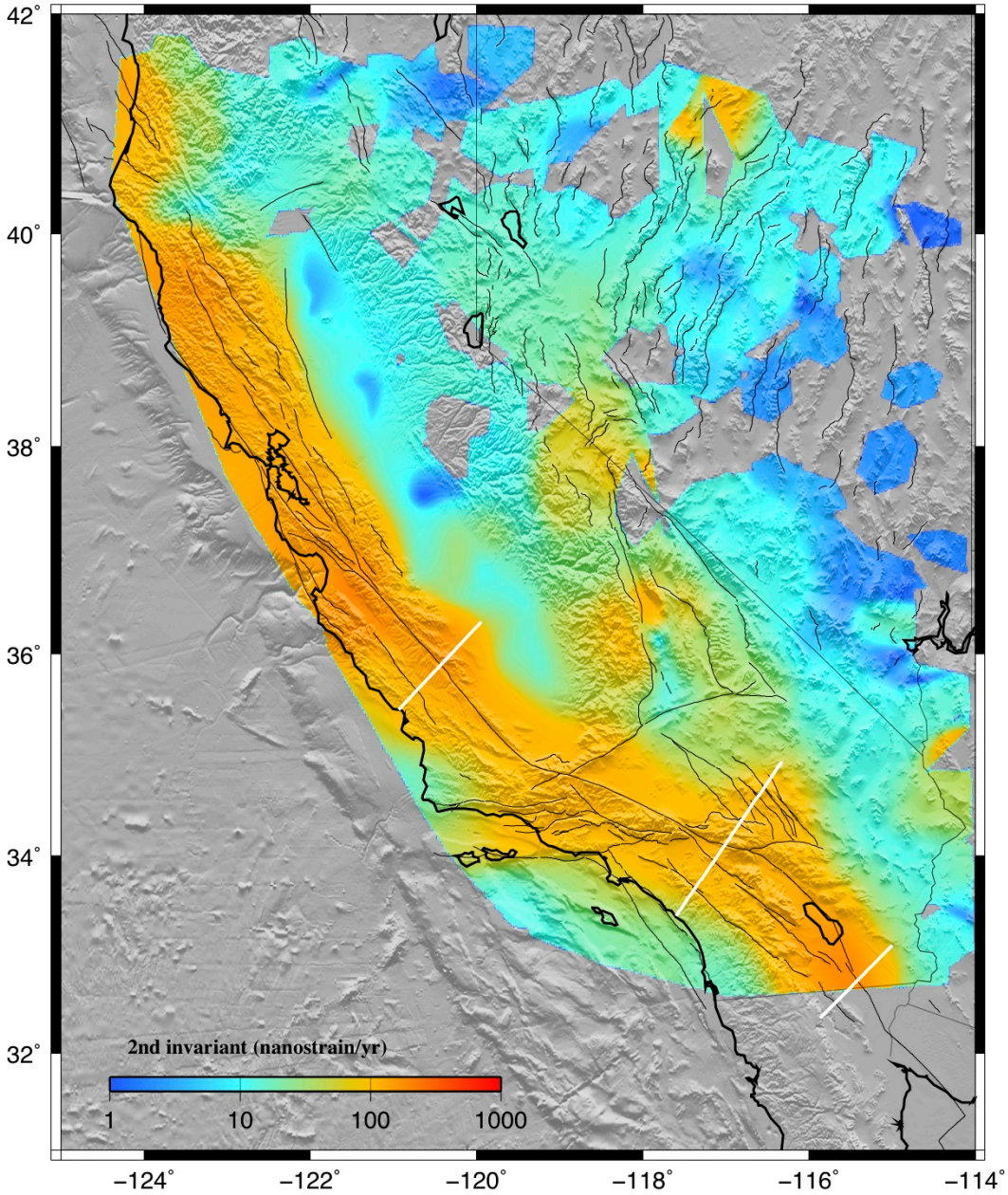

freed

Strain rates were derived based on 810 SCEC 3 velocity vectors (http://epicenter.usc.edu/cmm3/). We linearly interpolated the velocity data to an evenly spaced grid with increments of 0.1 degrees across the region using a weighted nearest neighboring scheme to dampen any locally sharp velocity contrasts. For grid points outside of the SCEC 3 region, we extrapolated the velocity field based on a fixed North America plate and a Pacific plate with a velocity of 48 mm/yr. We then triangulated the evenly spaced grid points using Delaunay triangulation (e.g., Shewchuk, 1996), and the strain tensor is determined for each triangle using minimum norm least squares. Reference: Freed et al., 2007.

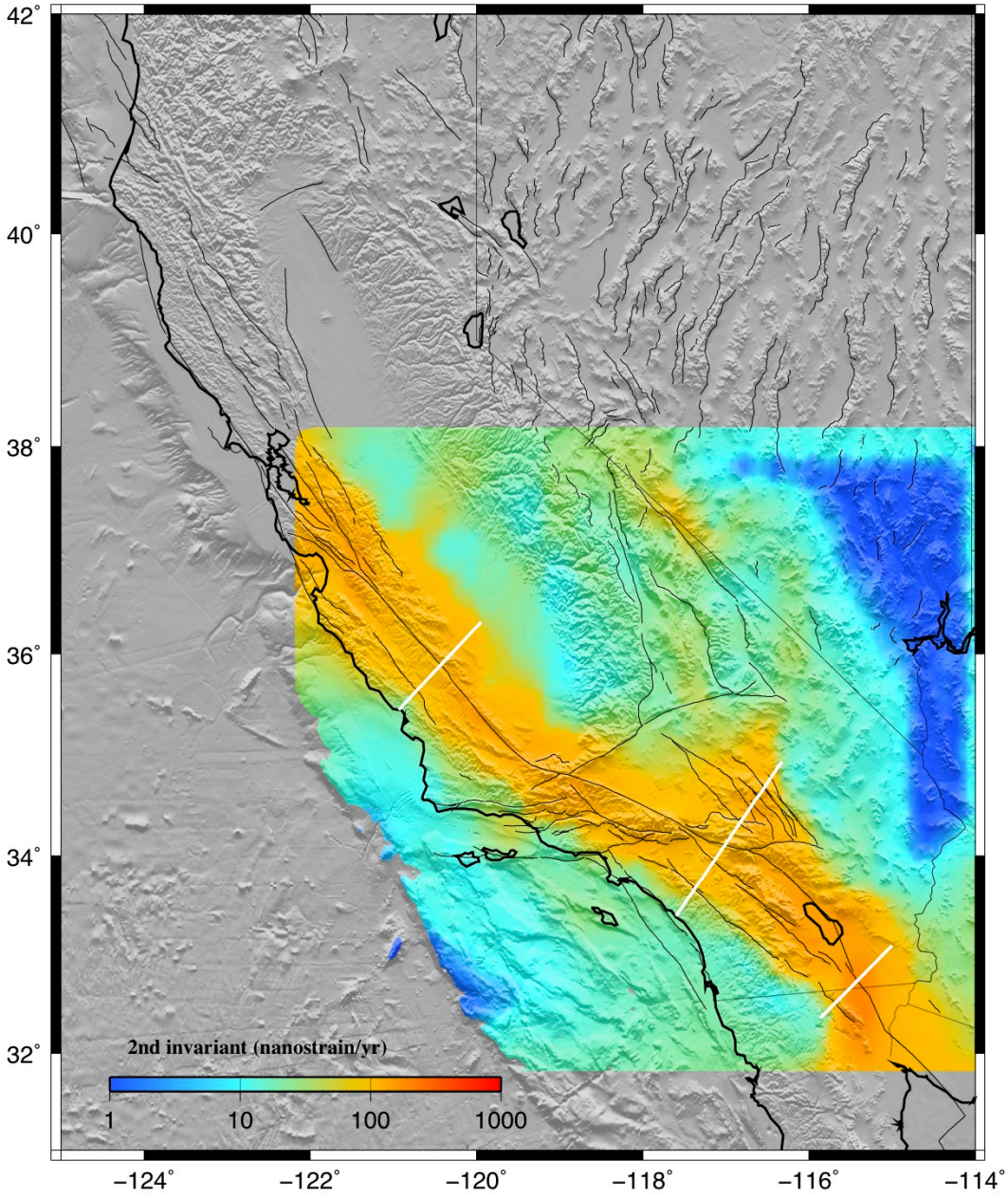

hooks

B.P. Hooks and B.R. Smith-Konter
Geological Sciences, Univ. of Texas – El Paso, El Paso, TX 79968

We present preliminary results of three-dimensional finite difference dynamic mechanical models. These models were completed using commercial software (Itasca, 2006; Fast Lagrangian Analysis of Continuum; FLAC^{3D}) that solves for large strains by utilizing simple stress – strain relationships and applied kinematic boundary conditions. The attached model results depart from a continuum through the inclusion of discontinuities that represent the major faults of the San Andreas Fault System. The model rheology is defined as a non-associated strain-weakening plasticity that allows for the localization of strain. A gridded PBO velocity is applied as a basal driving condition. The discontinuities behave according to the Coulomb sliding criteria and are assigned representative frictional properties. The solutions are produced through an explicit time-marching solution. The included data set (second invariant of the strain rate tensor; nanostrain/yr) is at 10 ky and at shallow depth (-2 km). Future iterations of this model will include dipping faults, topographically generated stress, pore fluid pressures, and temperature-dependent rheological models.

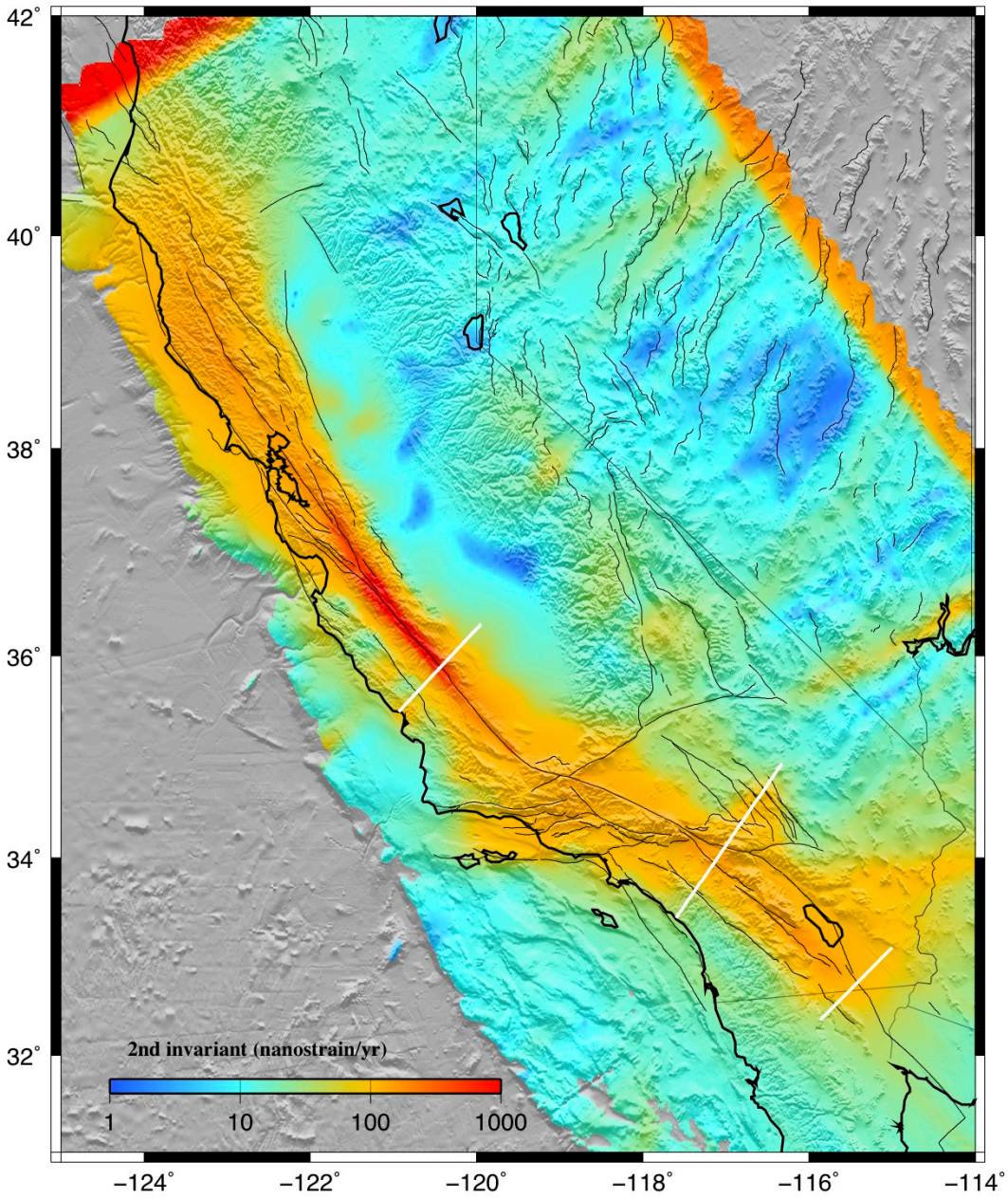

tape

Multiscale estimation of GPS velocity fields, C. Tape, P. Muse, M. Simons, D. Dong, and F. H. Webb, *Geophys. J. Int.*, 10.1111/j.1365-246X.2009.04337.x, 2009.

We present a spherical wavelet-based multiscale approach for estimating a spatial velocity field on the sphere from a set of irregularly spaced geodetic displacement observations. Because the adopted spherical wavelets are analytically differentiable, spatial gradient tensor quantities such as dilatation rate, strain rate and rotation rate can be directly computed using the same coefficients. In a series of synthetic and real examples,we illustrate the benefit of themultiscale approach, in particular, the inherent ability of the method to localize a given deformation field in space and scale as well as to detect outliers in the set of observations. This approach has the added benefit of being able to locally match the smallest resolved process to the local spatial density of observations, thereby both maximizing the amount of derived information while also allowing the comparison of derived quantities at the same scale but in different regions.We also consider the vertical component of the velocity field in our synthetic and real examples, showing that in some cases the spatial gradients of the vertical velocity field may constitute a significant part of the deformation. This formulation may be easily applied either regionally or globally and is ideally suited as the spatial parametrization used in any automatic time-dependent geodetic transient detector.

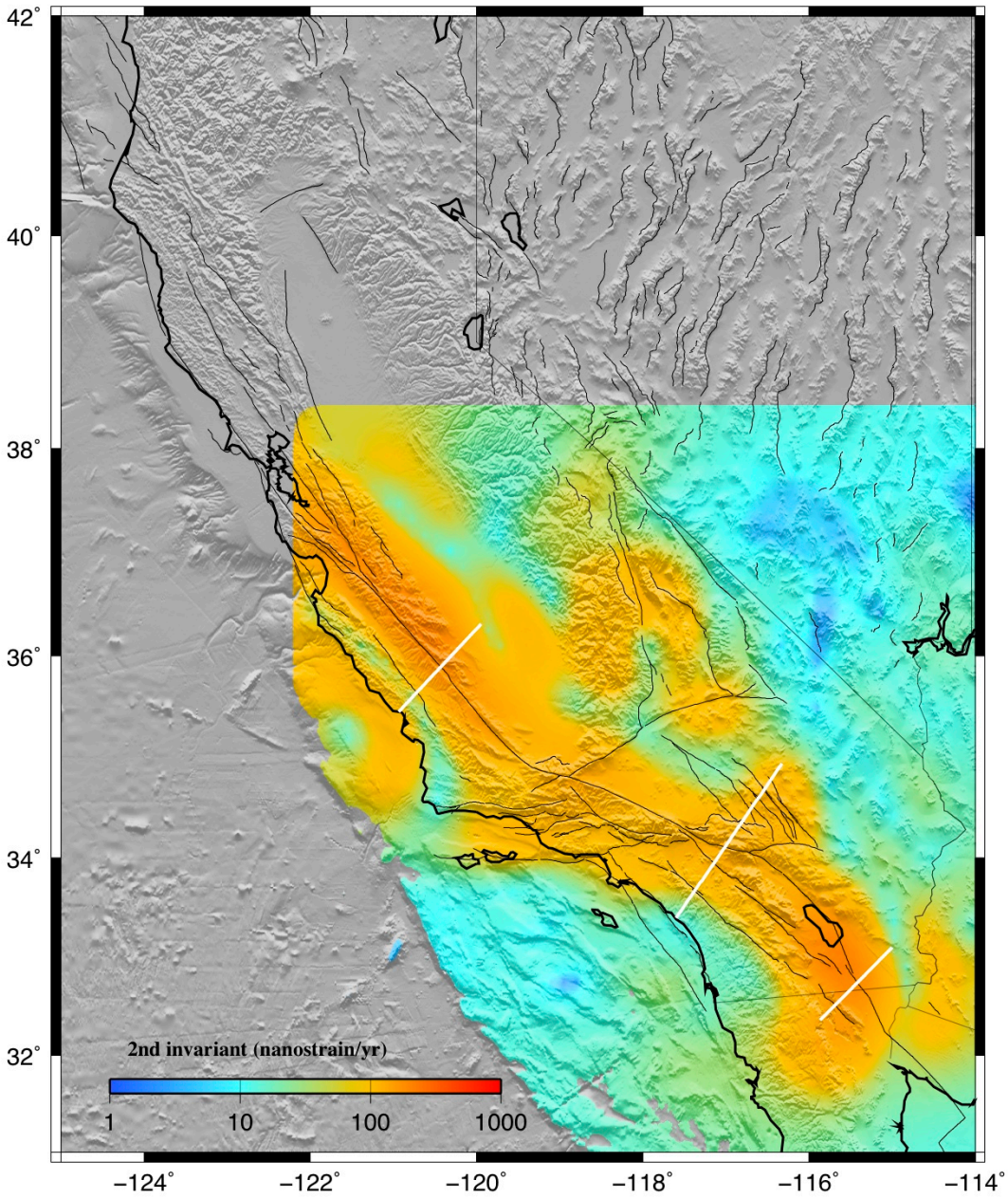

pollitz

Strain rates are derived by applying the isotropic interpolation method of Shen et al. (1996) to a compilation of 3650 horizontal GPS vectors in the western US. Contributing sources include PBO (714 vectors), Payne et al. (2008) (672 vectors), and various continuous and campaign GPS measurements (2264 vectors) such as USGS campaign data and the SCEC Crustal Motion Model 3.0. The Gaussian scaling distance used to weight velocity information in the Shen et al. method is here implemented as a function of position depending on the density of GPS measurements around a target point. This varies from 12 km in densely covered areas to 50 km in sparsely covered areas.

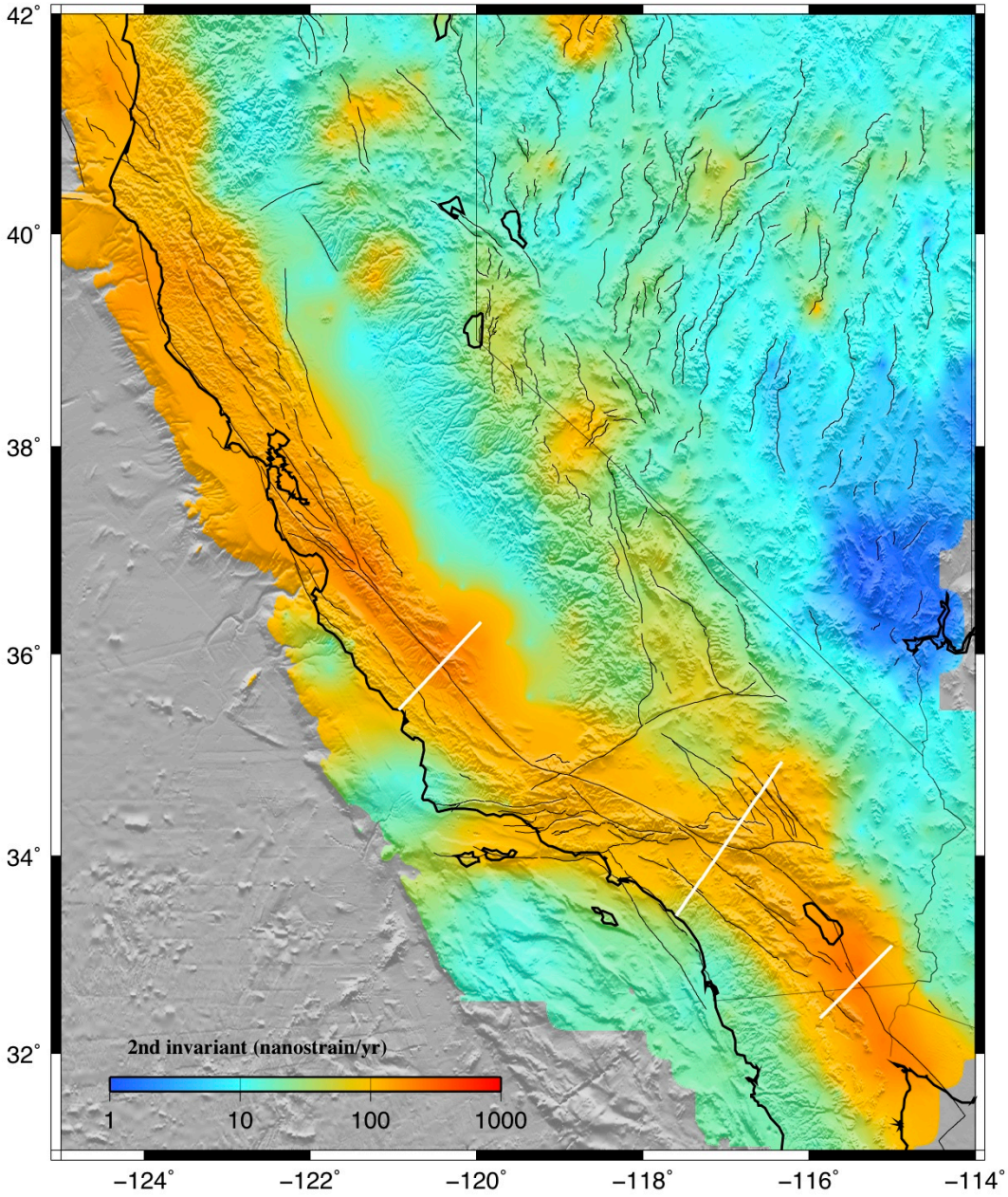

becker

Interpolated crustal strain rates based on the 20091130142023 releaseof the PBO GPS velocities, merged with the compilation by Kreemer andHammond (Geology, 2007). A high quality selection of data was used andprocessed via standard Generic Mapping Tools software (surface,grdfilter, grdgradient). The procedure follows that used in Platt etal. (EPSL, 2008), see that paper and Platt and Becker (submitted,2010; http://geodynamics.usc.edu/~becker/preprints/pb10.pdf)

fordetails.

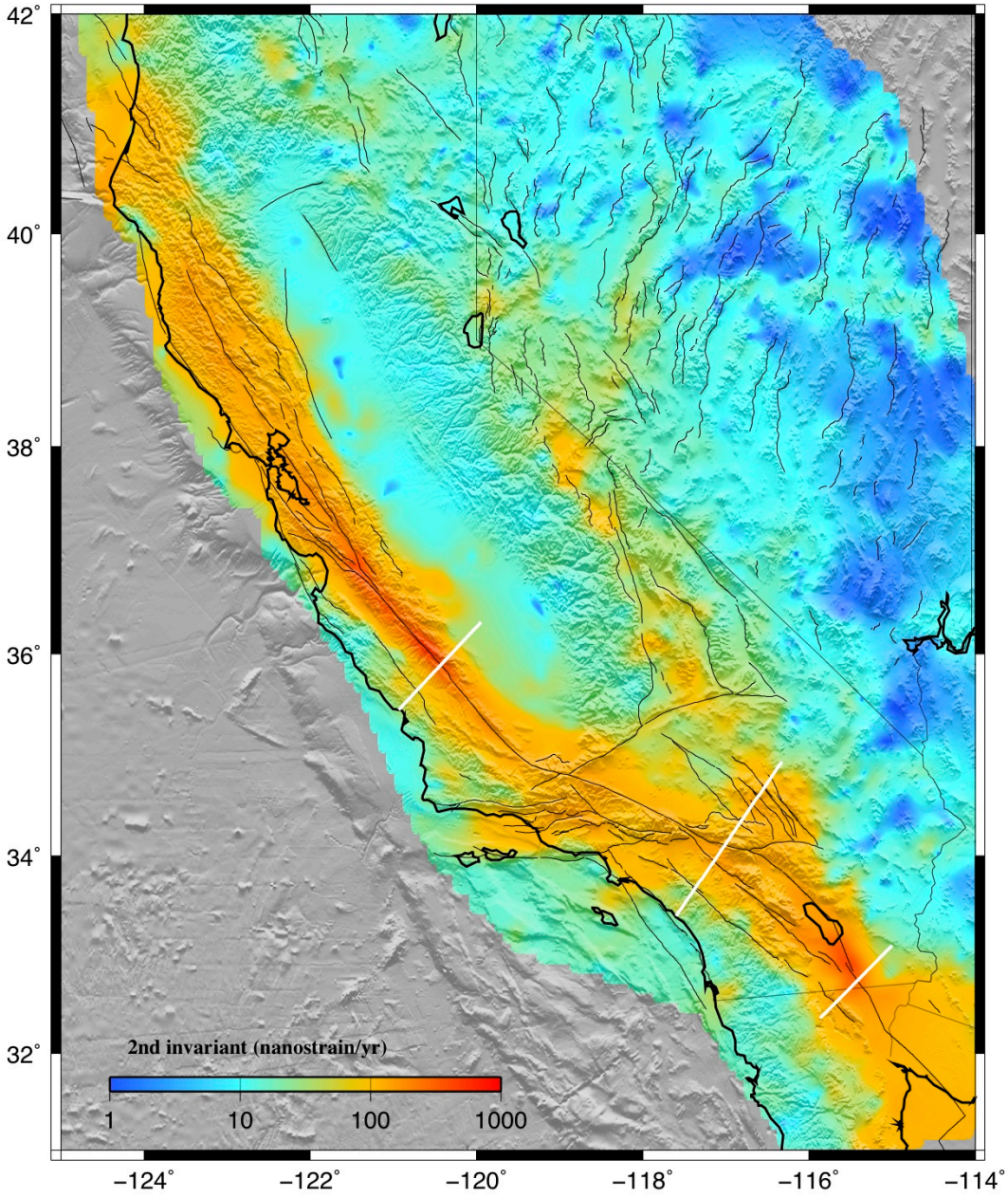

shen

Attached please find our data file. Interpolation is done using a weighting function†based on†azimuthal span and gaussian distance, and the decay distance constant is determined from a trade-off between the solution uncertainty and the weighting coefficient. Stations located in the 'shadow zone' behind the creeping section of the San Andreas are also screened out from the interpolation. The data file contains more items than you need, the ones relevant to your comparison are lat, lon, e11, e12, and e22.† '1' means east and '2' means north. You can discard the rest. Yuehua's solution submitted earlier was based on a slightly different approach, we will discuss the difference between that solution and†our current one in our presentation.† You may also enter both solutions in your comparisons if you like.

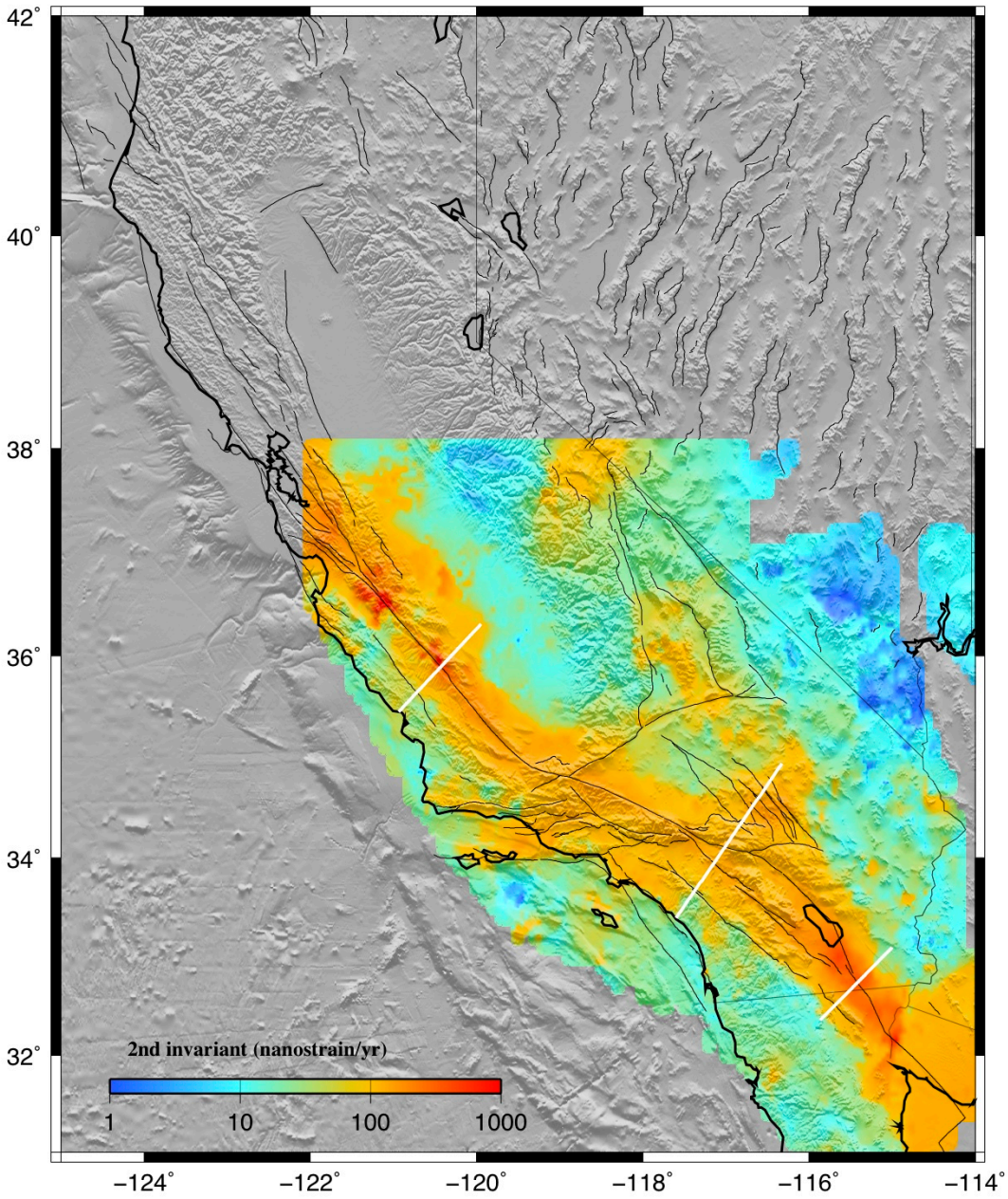

bormann

Jayne Bormann and Bill Hammond sent two velocity fields on a uniform grid constructed from their test exercise using CMM4. Here they are. One is for a block model with geologic slip constraints and the other is without geologic constraints.

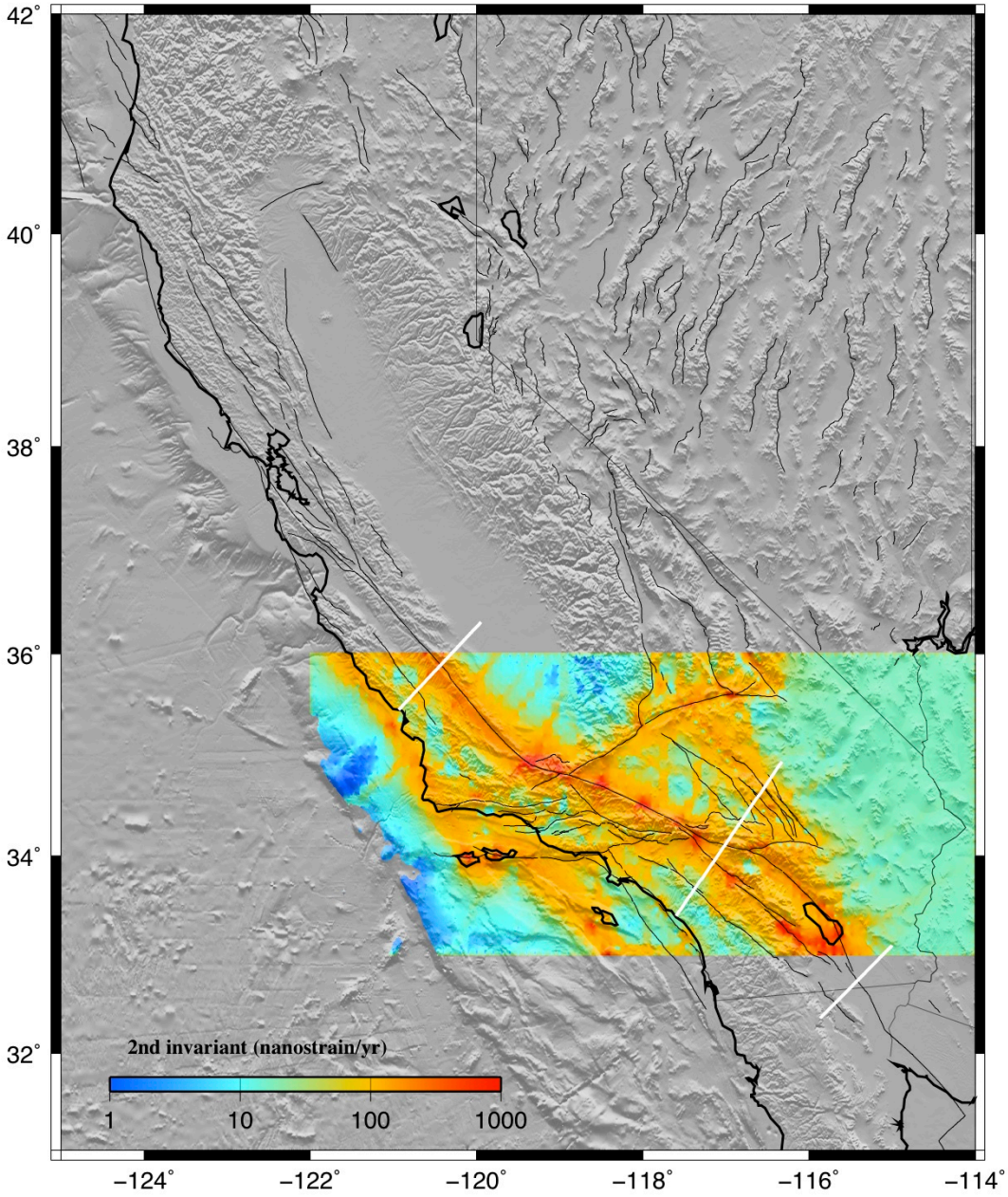

zeng

The GPS data for the western US are obtained from PBO velocity at UNAVCO site, Southern California Earthquake Center California Crustal Motion Map 1.0, McCaffrey et al. (2007) for Pacific Northwest, the GPS velocity field of Nevada and its surrounding area from the Nevada Geodetic Lab at the University of Nevada at Reno, and the GPS velocity field of the Wasatch-Front and the Yellowstone-Snake-River-River-Plain network from Bob Smith of University of Utah. These separate velocity fields are combined by adjusting their reference frames to make velocities match at collocated stations. I determined the Voronoi cells for this combined GPS stations and used their areas to weight the corresponding stations for inversion. I then interpolated those GPS observation into uniform grid point for the western US using the method of Wald (1998) and calculated the final strain rate map.

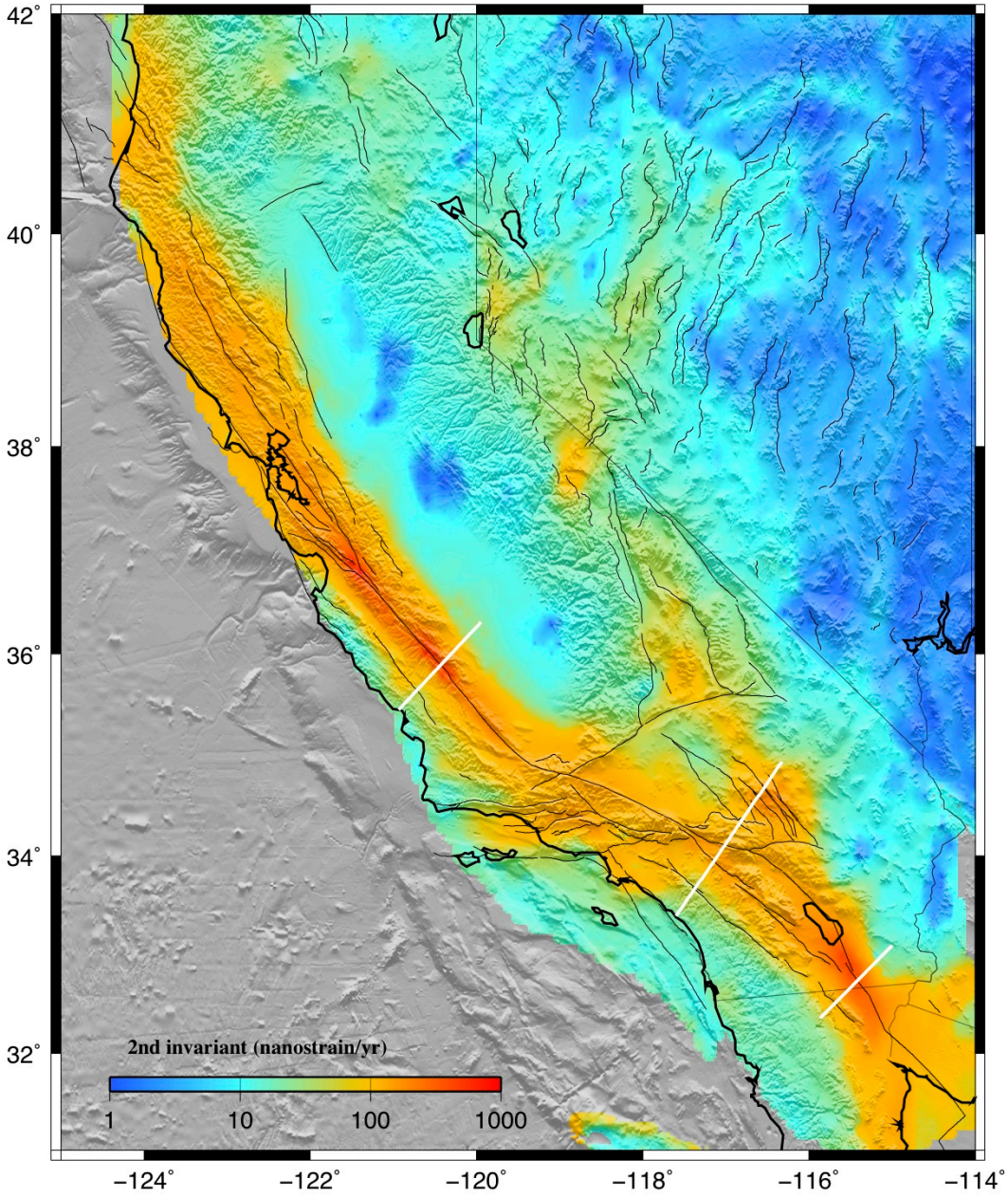

parsons

Tectonic stressing in California modeled from GPS observations Parsons,Tom Journal of Geophysical Research, Volume 111, Issue B3, CiteID B03407

What happens in the crust as a result of geodetically observed secular motions? In this paper we find out by distorting a finite element model of California using GPS-derived displacements. A complex model was constructed using spatially varying crustal thickness, geothermal gradient, topography, and creeping faults. GPS velocity observations were interpolated and extrapolated across the model and boundary condition areas, and the model was loaded according to 5-year displacements. Results map highest differential stressing rates in a 200-km-wide band along the Pacific-North American plate boundary, coinciding with regions of greatest seismic energy release. Away from the plate boundary, GPS-derived crustal strain reduces modeled differential stress in some places, suggesting that some crustal motions are related to topographic collapse. Calculated stressing rates can be resolved onto fault planes: useful for addressing fault interactions and necessary for calculating earthquake advances or delays. As an example, I examine seismic quiescence on the Garlock fault despite a calculated minimum 0.1-0.4 MPa static stress increase from the 1857 M~7.8 Fort Tejon earthquake. Results from finite element modeling show very low to negative secular Coulomb stress growth on the Garlock fault, suggesting that the stress state may have been too low for large earthquake triggering. Thus the Garlock fault may only be stressed by San Andreas fault slip, a loading pattern that could explain its erratic rupture history.

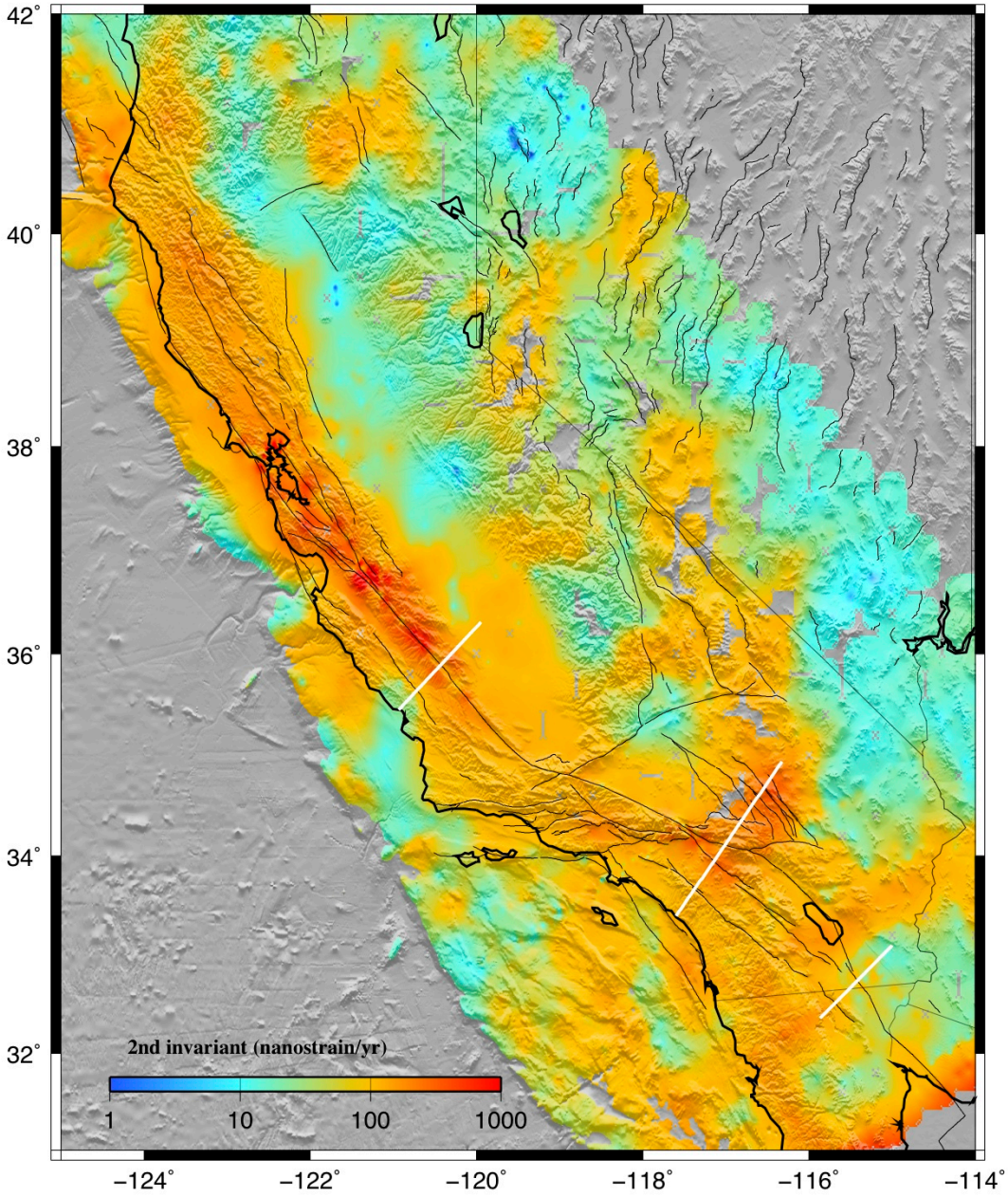

holt

What I do is use an anisotropic variance-covariance matrix for the strain rates. I do not build in fault slip rates, but I use the variance-covariance matrix to place a priori constraints on expected shear directions as well as some constraints on expected shear magntitudes. However, in the end the GPS velocities dictate the actual strain rates and styles of strain rate (where they are high, low, etc.). I am also limited by the finite-element grid, which is .1x.1 degree grid area spacing. It might be worthwhile to compare the solution I sent you with one obtained using fully isotropic uniform variances for all areas. That is, with an a priori expected strain rate distribution that is everywhere uniform. I can look into the reduced chi-squared misfit for both of these

cases.

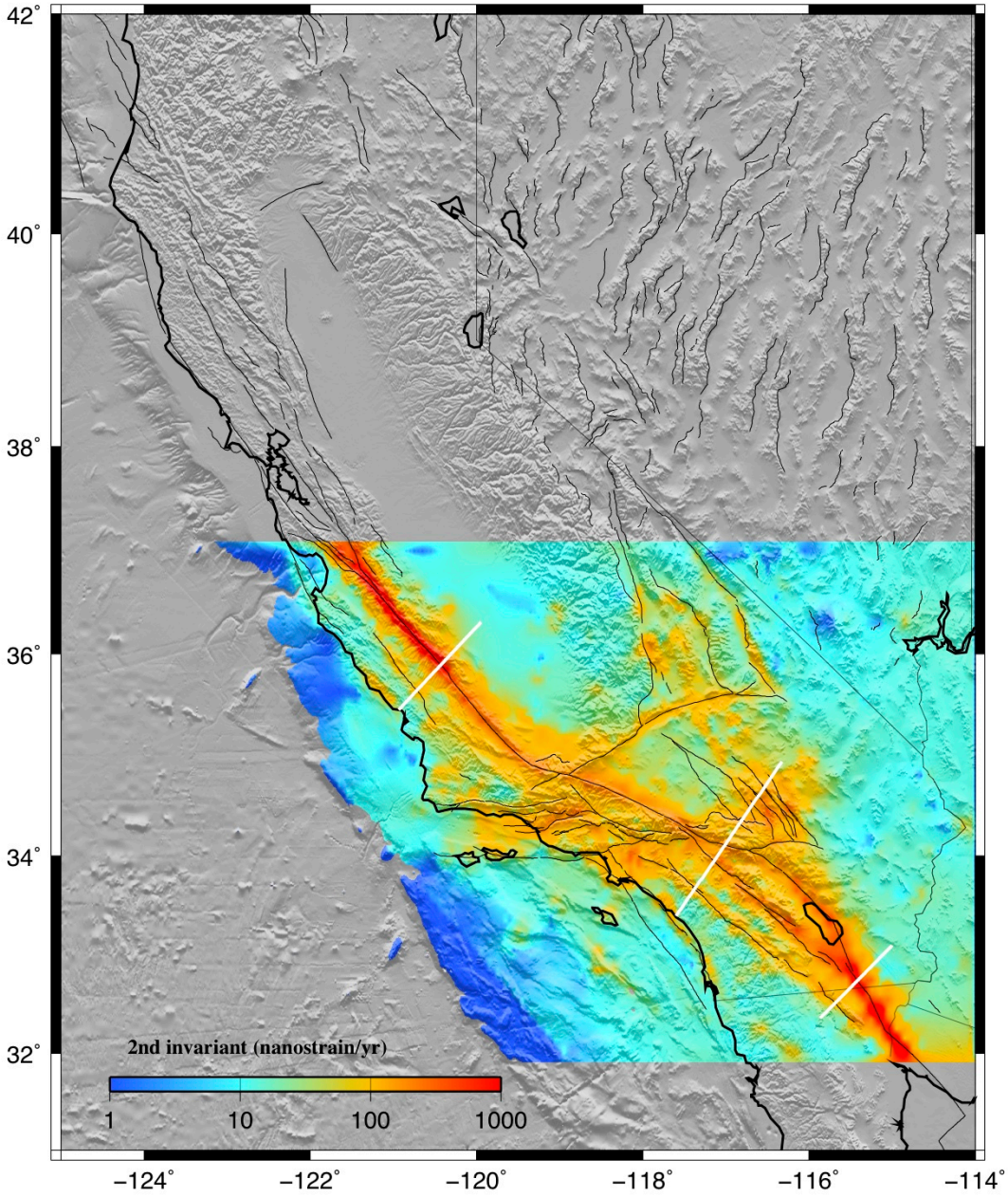

kreemer

Strain rate tensor model derived from fitting a continuous horizontal velocity field through GPS velocities [Kreemer et al, 2009, this meeting]. 2053 GPS velocities were used, of which 854 from our own analysis of (semi-)continuous sites and 1199 from published campaign measurements (all transformed into the same reference frame). The model assumes that the deformation is accommodated continuously, and lateral variation in damping is applied to ensure that the reduced chi^2 fit between observed and modeled velocities is ~1.0 for subregions.

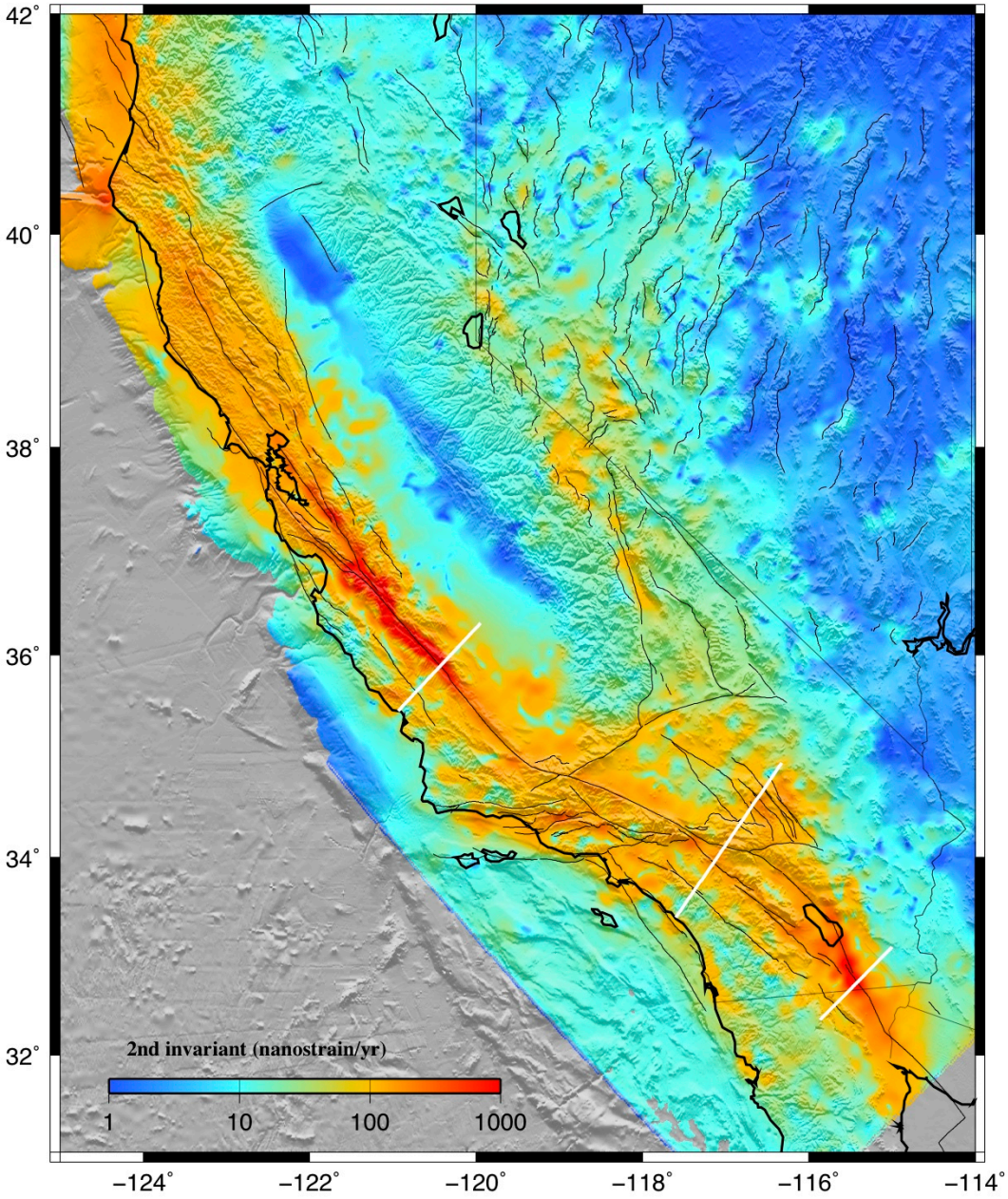

smith_konter

Strain rate derived from a dislocation model of the San Andreas Fault system [Smith-Konter and Sandwell, GRL, 2009]. 610 GPS velocity vectors were used to develop the model. The model consists of an elastic plate over a visco-elastic half space at 1 km horizontal resolution. Deep slip occurs on 41 major fault segments where rate is largely derived from geological studies. The locking depth is varied along each fault segment to provide a best fit to the GPS data. The model is fully 3-D and the vertical component of the GPS vectors is also used in the adjustment. An additional velocity model was developed by gridding the residuals to the GPS data using the GMT surface program with a tension of 0.35. This was added to the dislocation model.

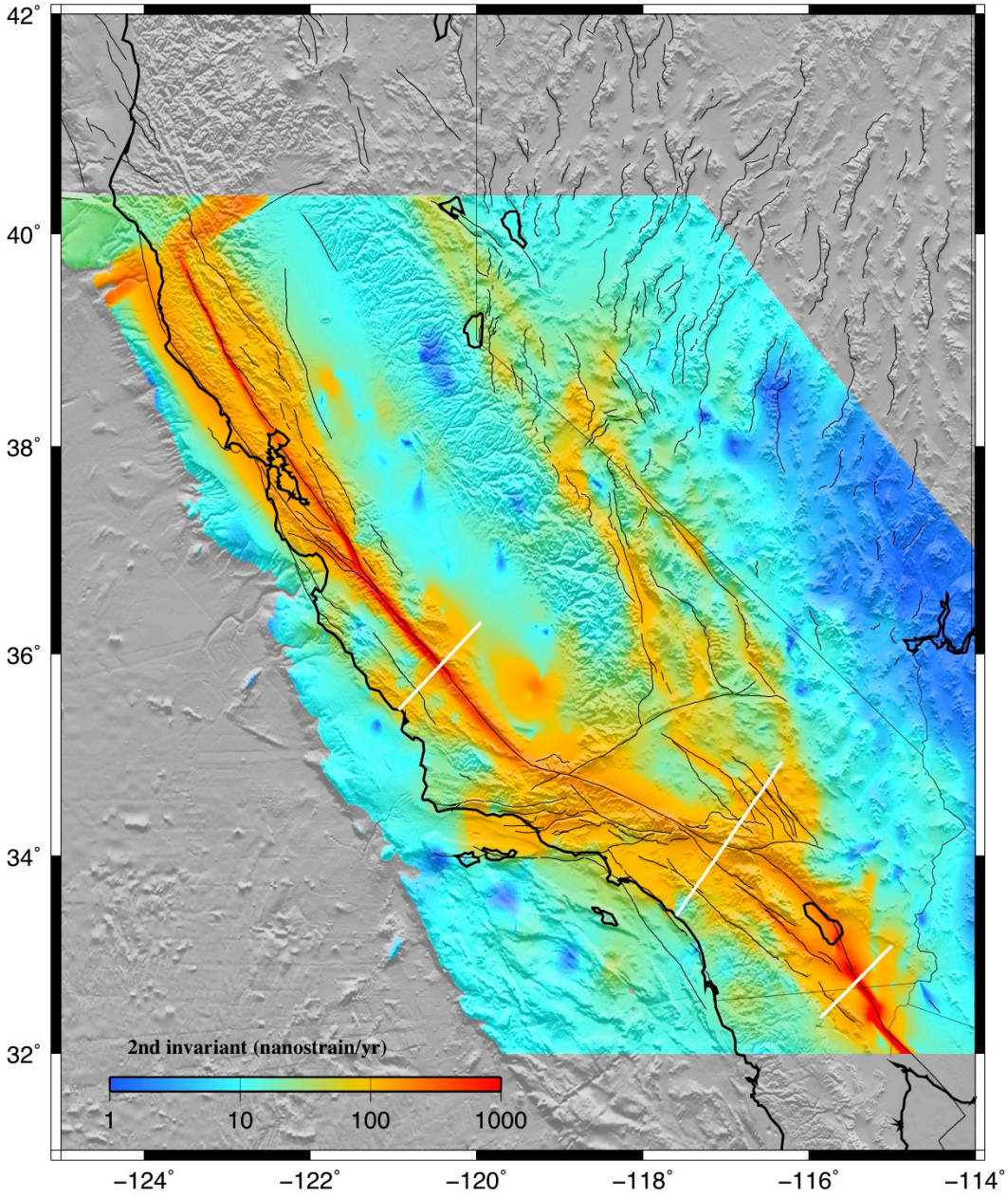

harvard

The strains are calculated analytically using elastic dislocation theory in a homogeneous elastic halfspace. The model is subset of a western US block model geodetically constrained by a combination of the SCEC CMM 3.0, McClusky ECSZ, Hammond Walker Lane, McCaffrey PNW, d'Allessio Bay Area, and PBO velocity fields. These are combined by minimizing residuals (6-parameter) at collocated stations. In southern California the block geometry is based on and the Plesch et al., CFM-R and features dipping faults in the greater Los Angeles regions which end up producing some intricate strain rate patterns. The model features fully coupled (locked from the surface to some locking depth) faults everywhere except for Parkfield, the SAF just north, and the Cascadia subduction zone. For Parkfield and Cascadia we solve for smoothly varying slip on surfaces parameterized using triangular dislocation elements.

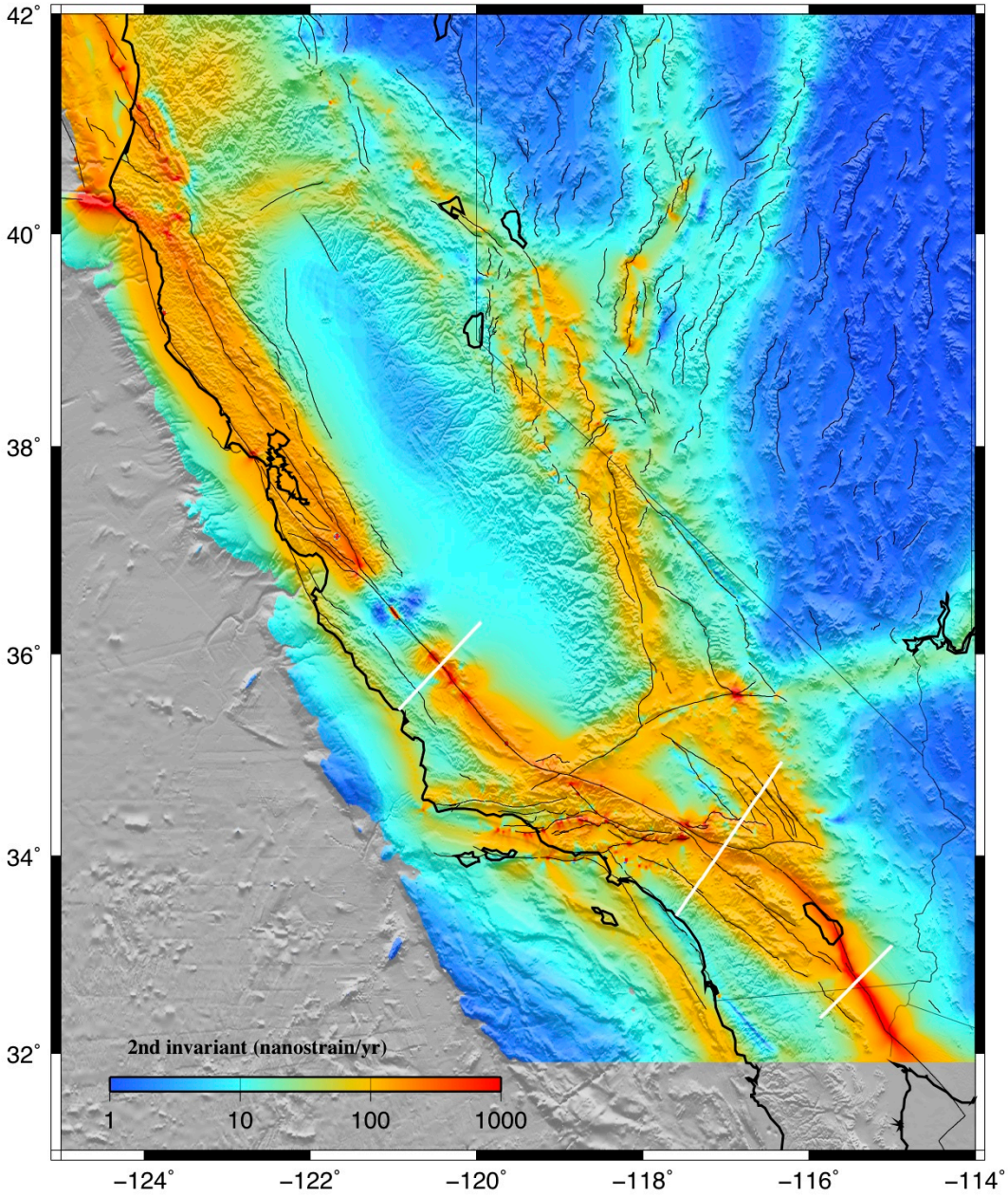

mccaffrey

Model of horizontal surface velocities (converted to strain) for the western United States. While there are many ways to go about doing this, here we have chosen to generate a geologic block model, constrained by observations from geodesy, seismology and geology. The parameters of the block model are constrained by non-linear least-squares inversion. The locking depth is set to 10 km for segments where locking depth is not well constrained by GPS. The model is used to predict surface velocity on a uniform grid at 0.02 degree spacing. Grids were filtered at 0.5 gain at 10 km wavelength.

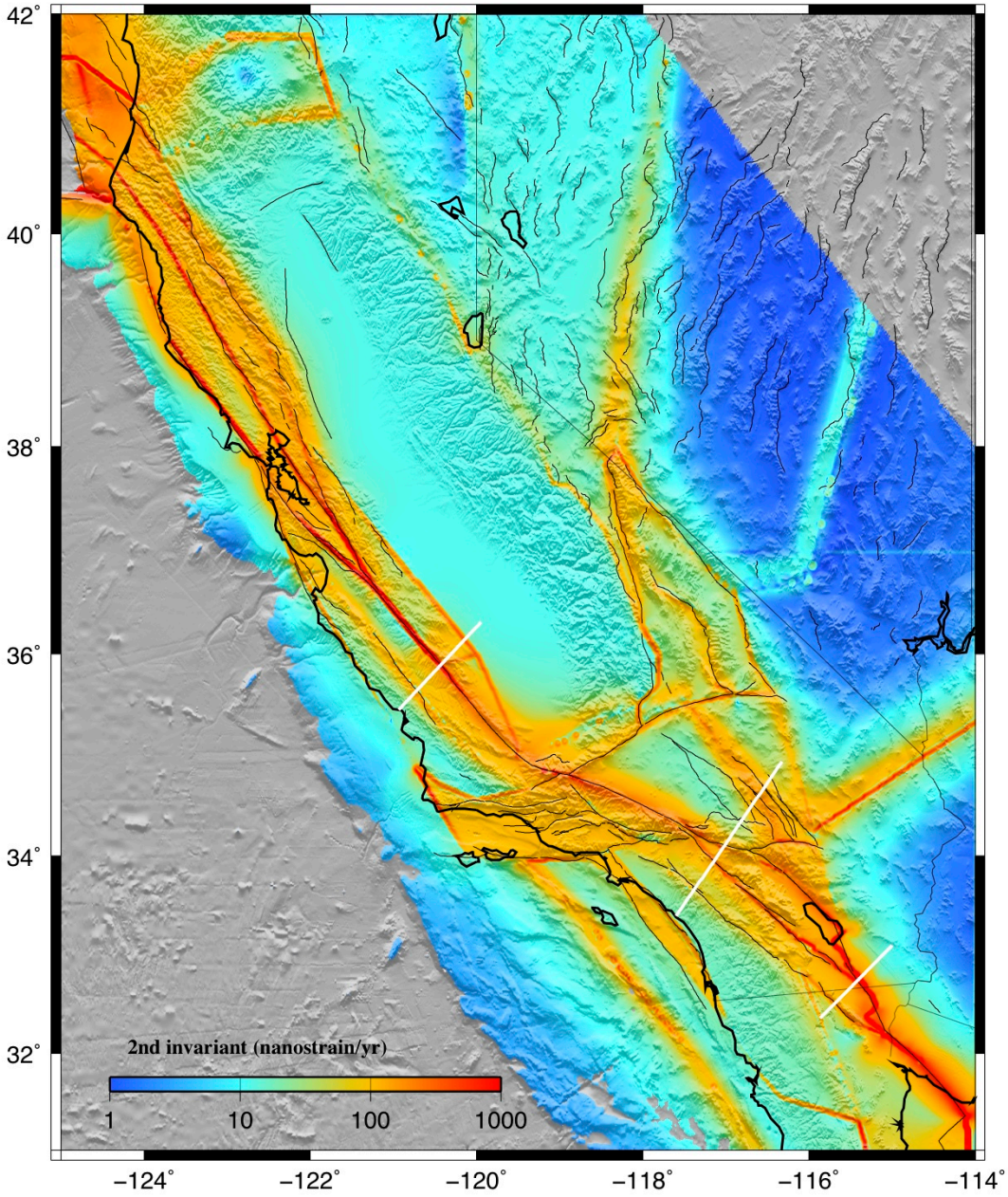

bird

Attached are my interseismic strain-rate results for two NeoKinema models of the southern California comparison test exercise:

NeoKinema_composite_interseismic_strain_rate.zip
is my best/preferred composite model, using both the GPS rates provided and "my own" [Bird, 2007, 2009] geologic offset rates.

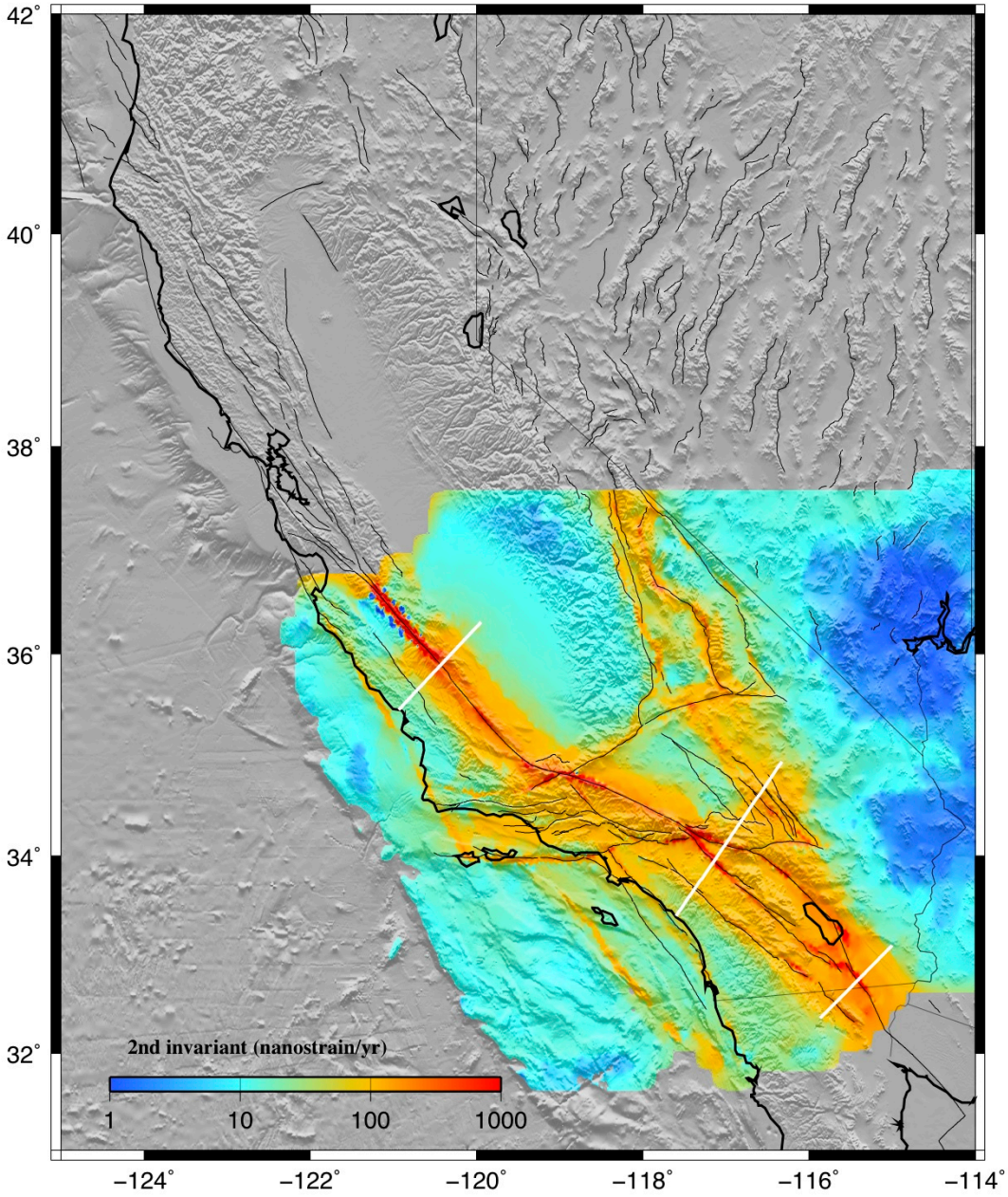

UCERF

The colors on this California map represent the UCERF probabilities of having a nearby earthquake rupture (within 3 or 4 miles) of magnitude 6.7 or larger in the next 30 years. As shown in the table, the chance of having such an event somewhere in California exceeds 99%. The 30-year probability of an even more powerful quake of magnitude 7.5 or larger is about 46%.

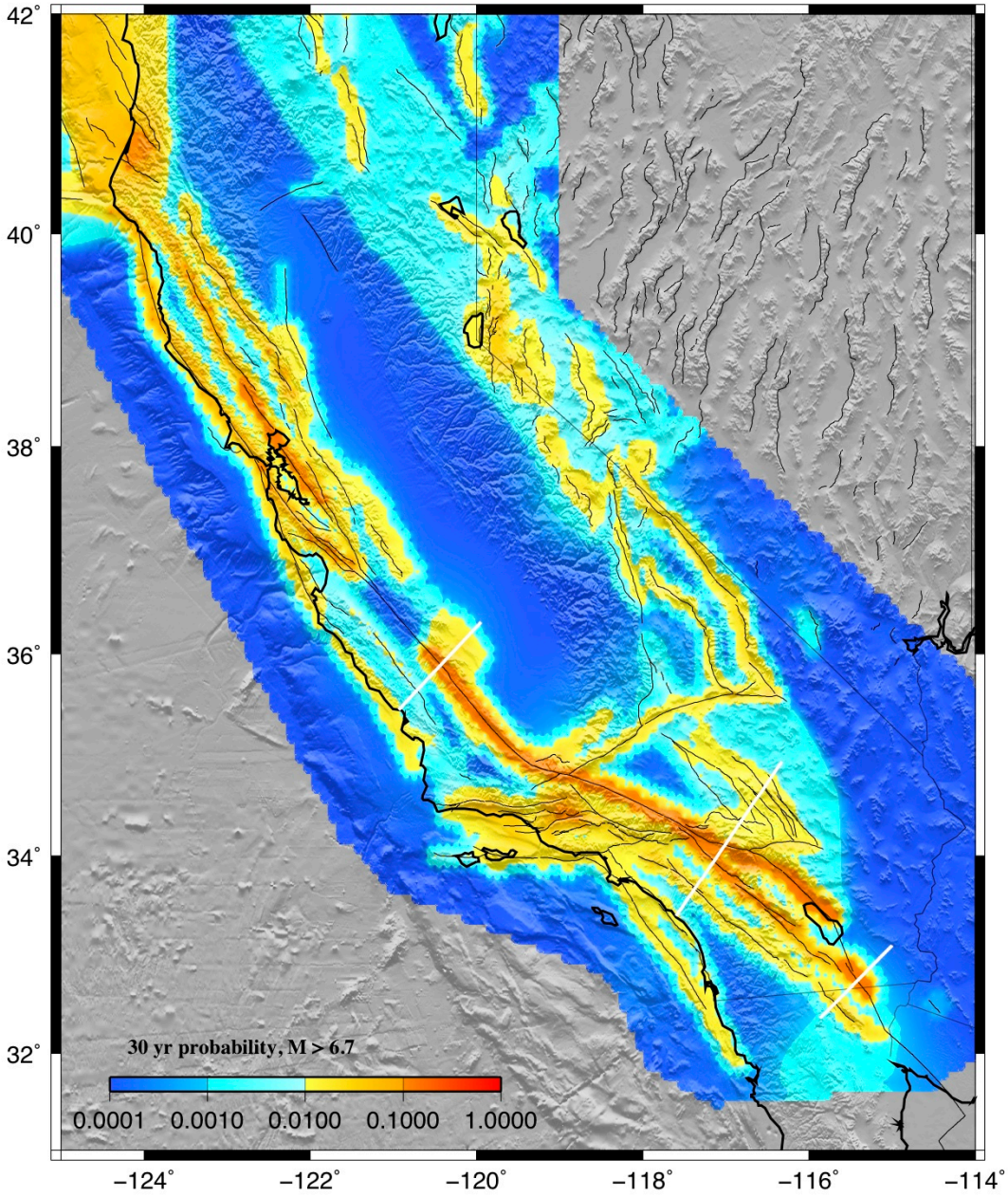

What is the true strain rate?

Profiles of strain rate across the San Andreas Fault at three locations. (upper) profiles cross the Parkfield area where there is dense GPS coverage. (middle) profiles across the Los Angeles Basin, and Mojave region where GPS spacing is highly non-uniform. (lower) profiles across the Imperial fault where campaign GPS coverage is very dense.

Note the largest differences in strain rate occur within 15 km of the San Andreas fault zone.

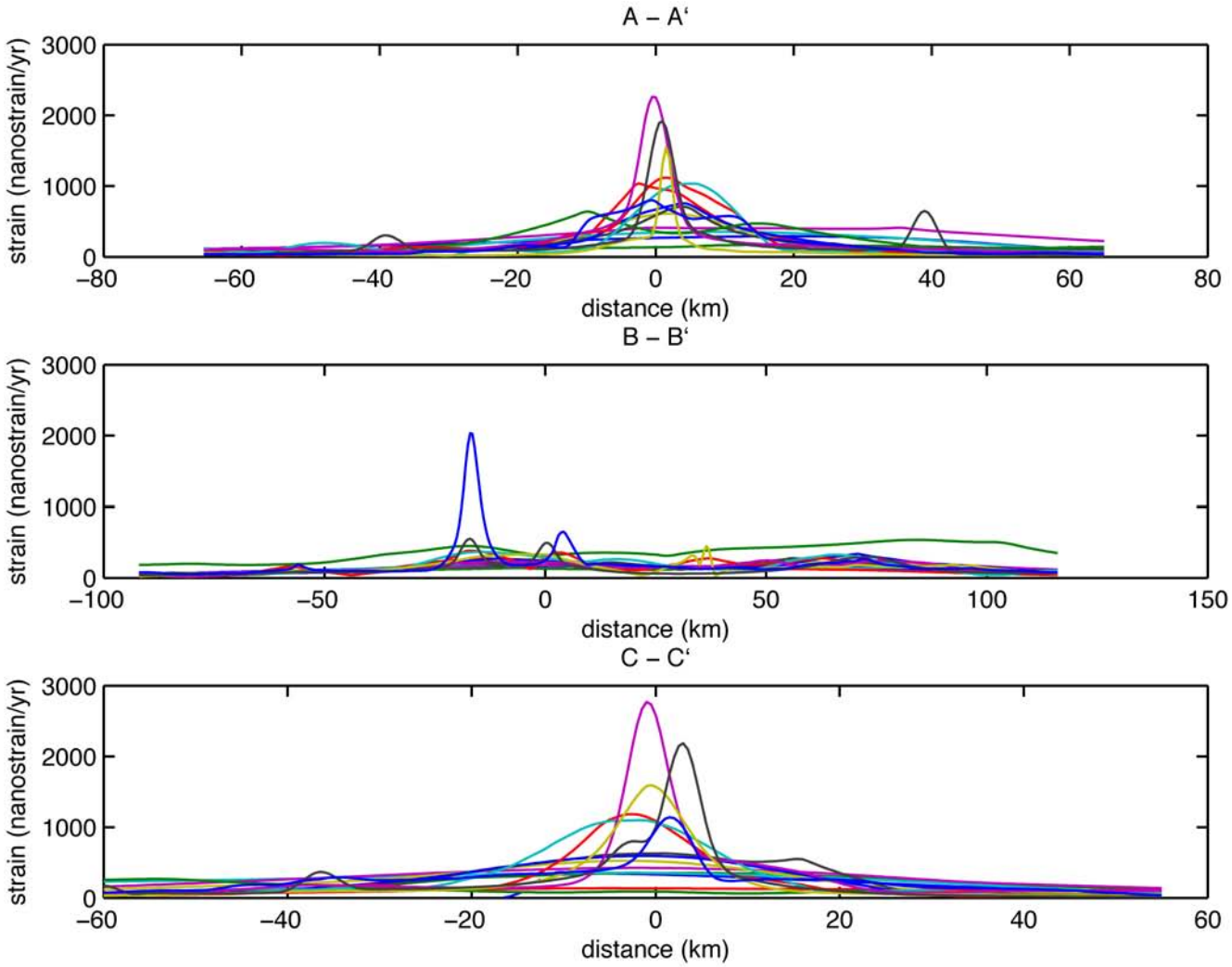

freed

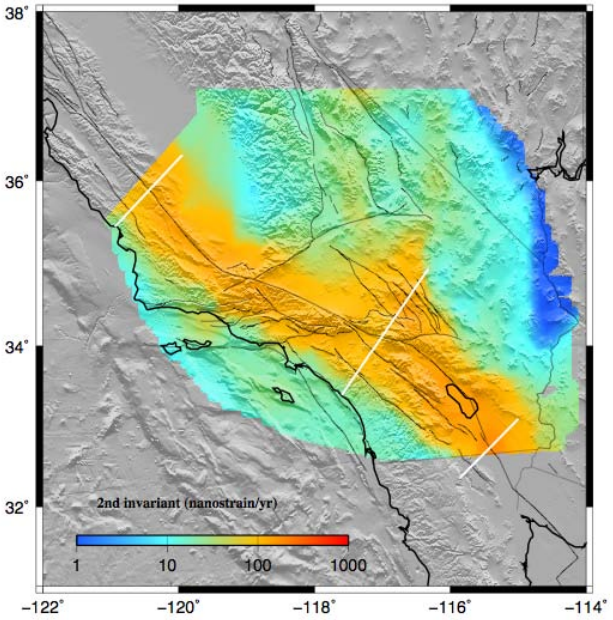

shen

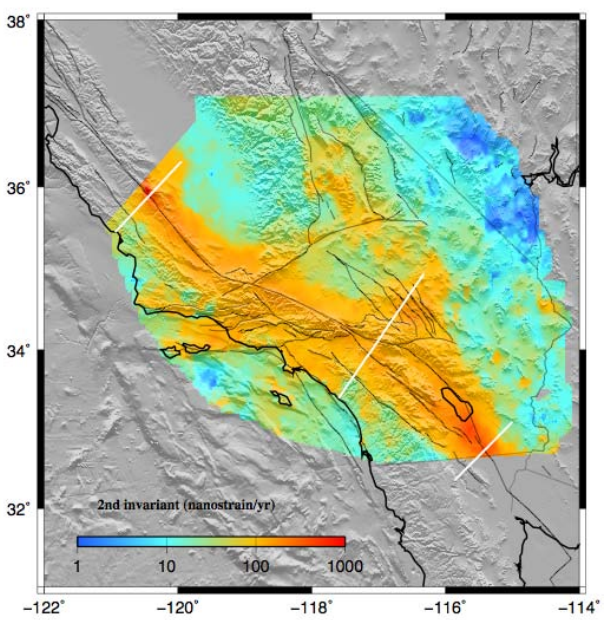

holt

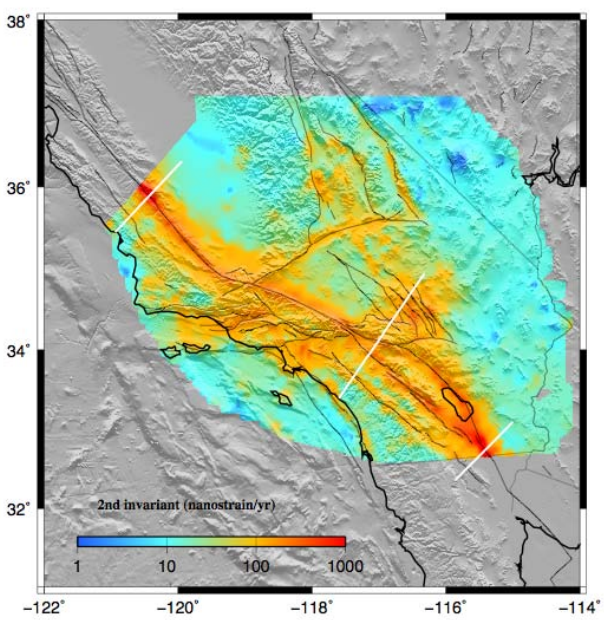

harvard

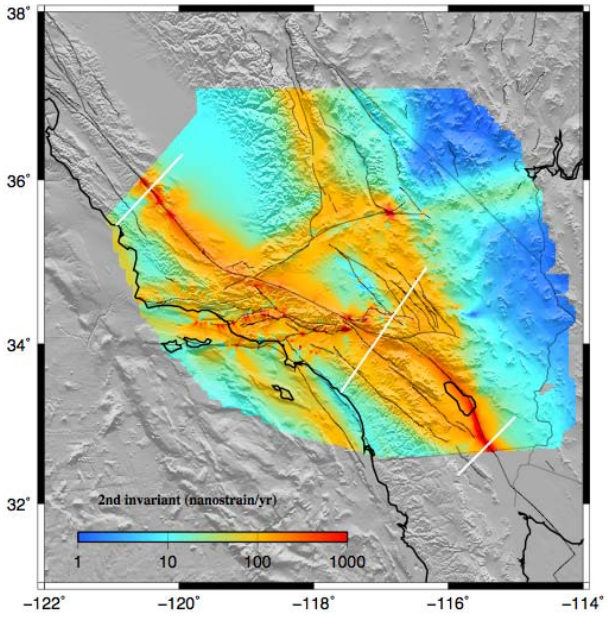

bird

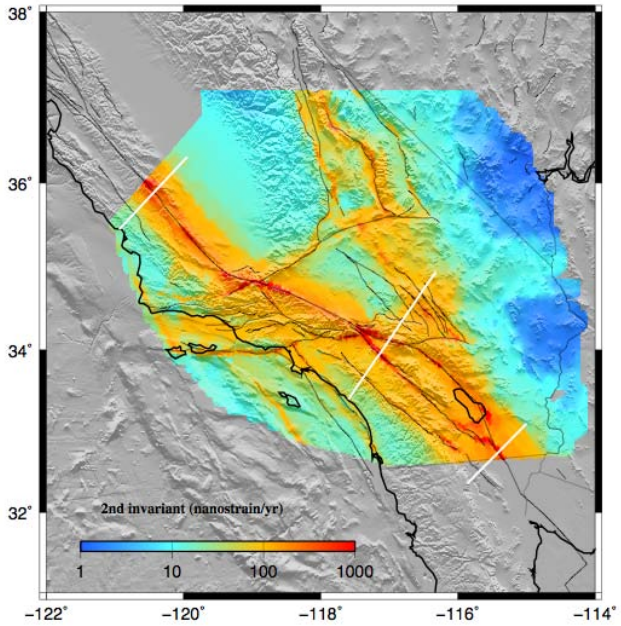

UCERF

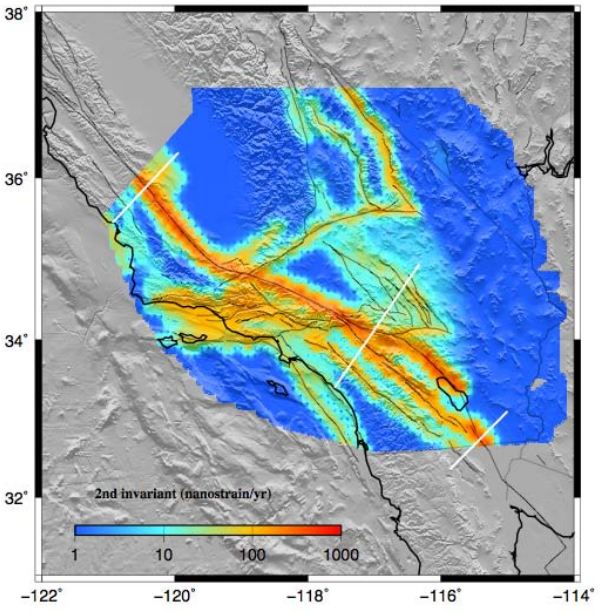

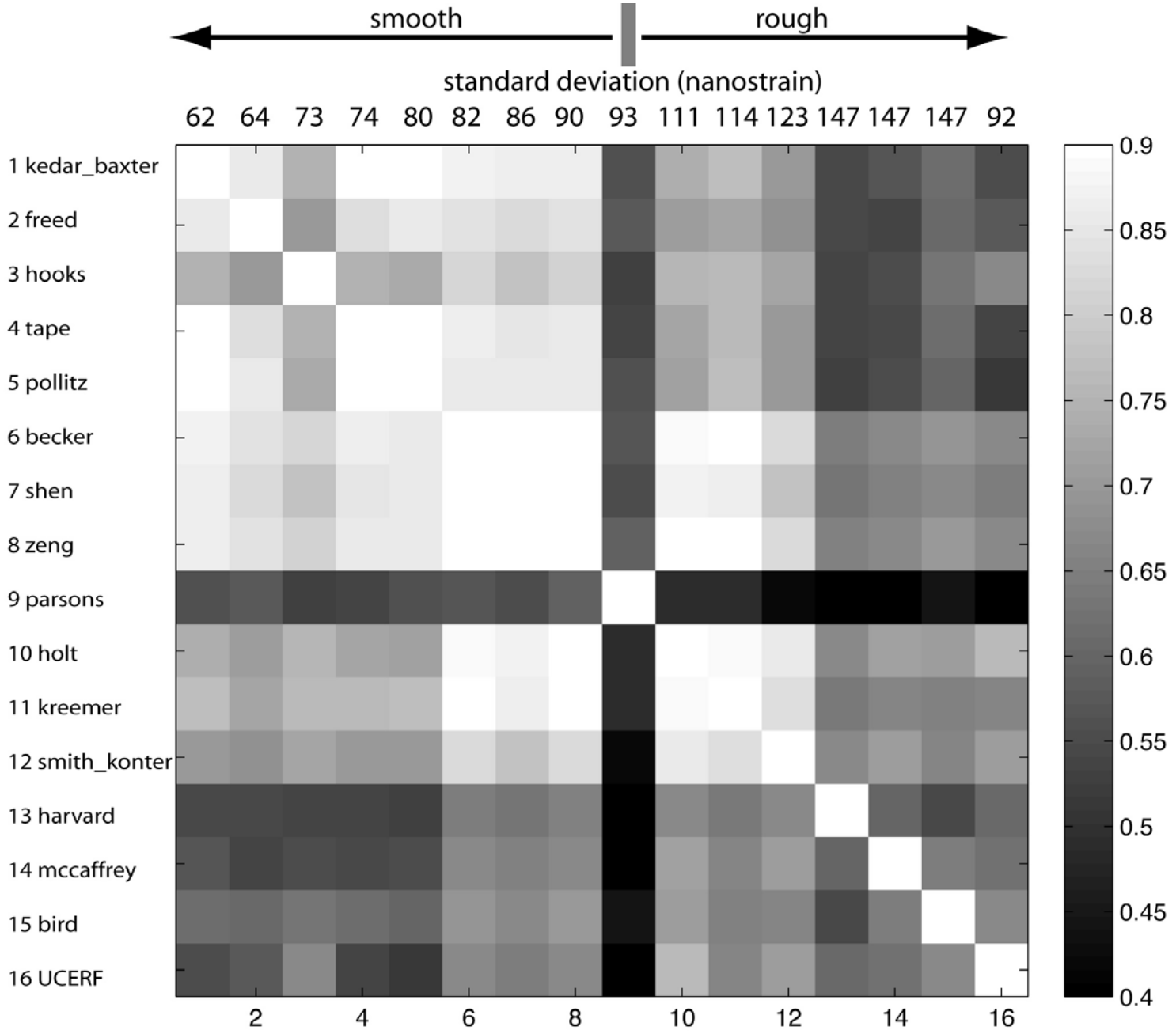
smooth
rough
standard deviation (nanostrain)
62 64 73 74 80 82 86 90 93 111 114 123 147 147 147 92
1 kedar_baxter
2 freed
3 hooks
4 tape
5 pollitz
6 becker
7 shen
8 zeng
9 parsons
10 holt
11 kreemer
12 smith_konter
13 harvard
14 mccaffrey
15 bird
16 UCERF
2 4 6 8 10 12 14 16
0.9
0.85
0.8
0.75
0.7
0.65
0.6
0.55
0.5
0.45
0.4

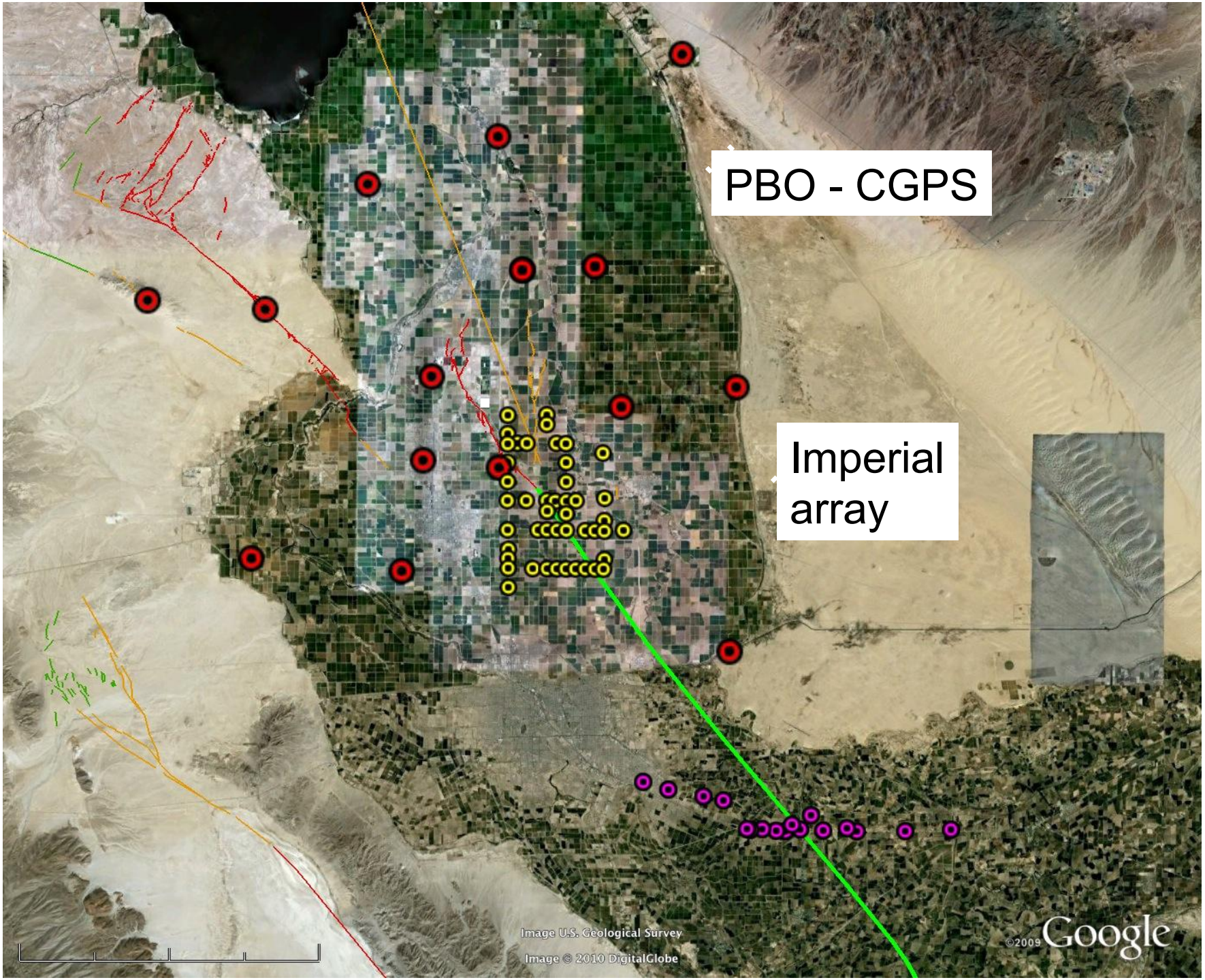
PBO - CGPS
Imperial array
Image U.S. Geological Survey
Image © 2010 DigitalGlobe
©2009 Google

Imperial array

High density campaign GPS measurements across the Imperial fault provide the data needed to estimate the strain rate [Lyons et al., 2002]. The best-fit 2-D dislocation model has a velocity V_o of 40 mm/yr and a locking depth d of 6 km (upper plot). The derivative of this velocity profile provides the shear strain rate (lower plot). The peak strain rate is given by

$$\dot{\varepsilon} = \frac{V}{\pi D}$$

which in this case has a value of 2120 nanostrain/yr.

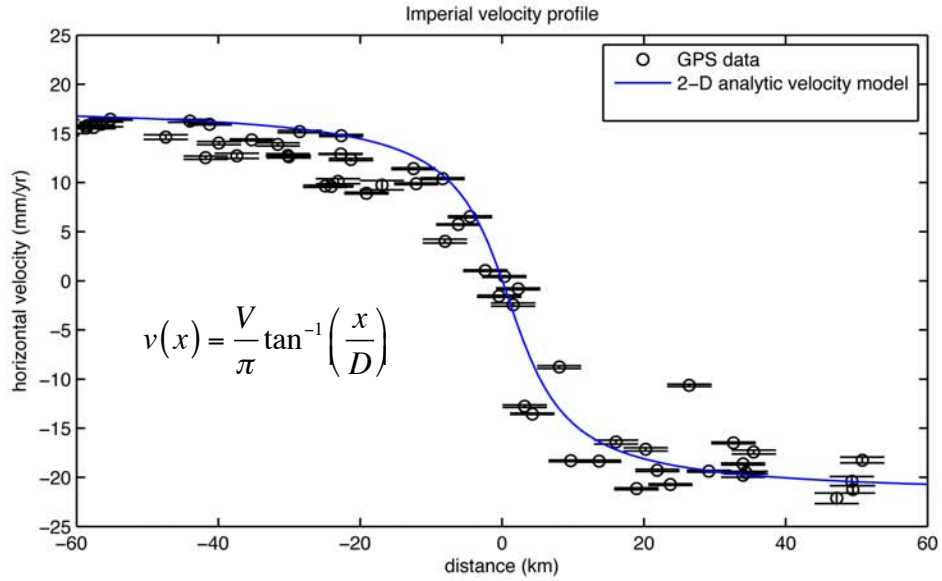

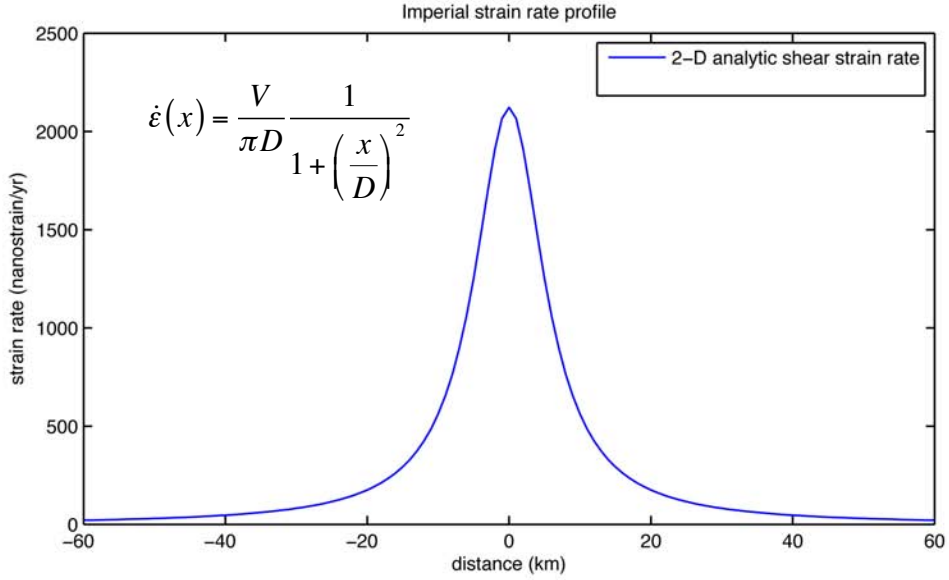

strain rate > 1000 at Imperial array

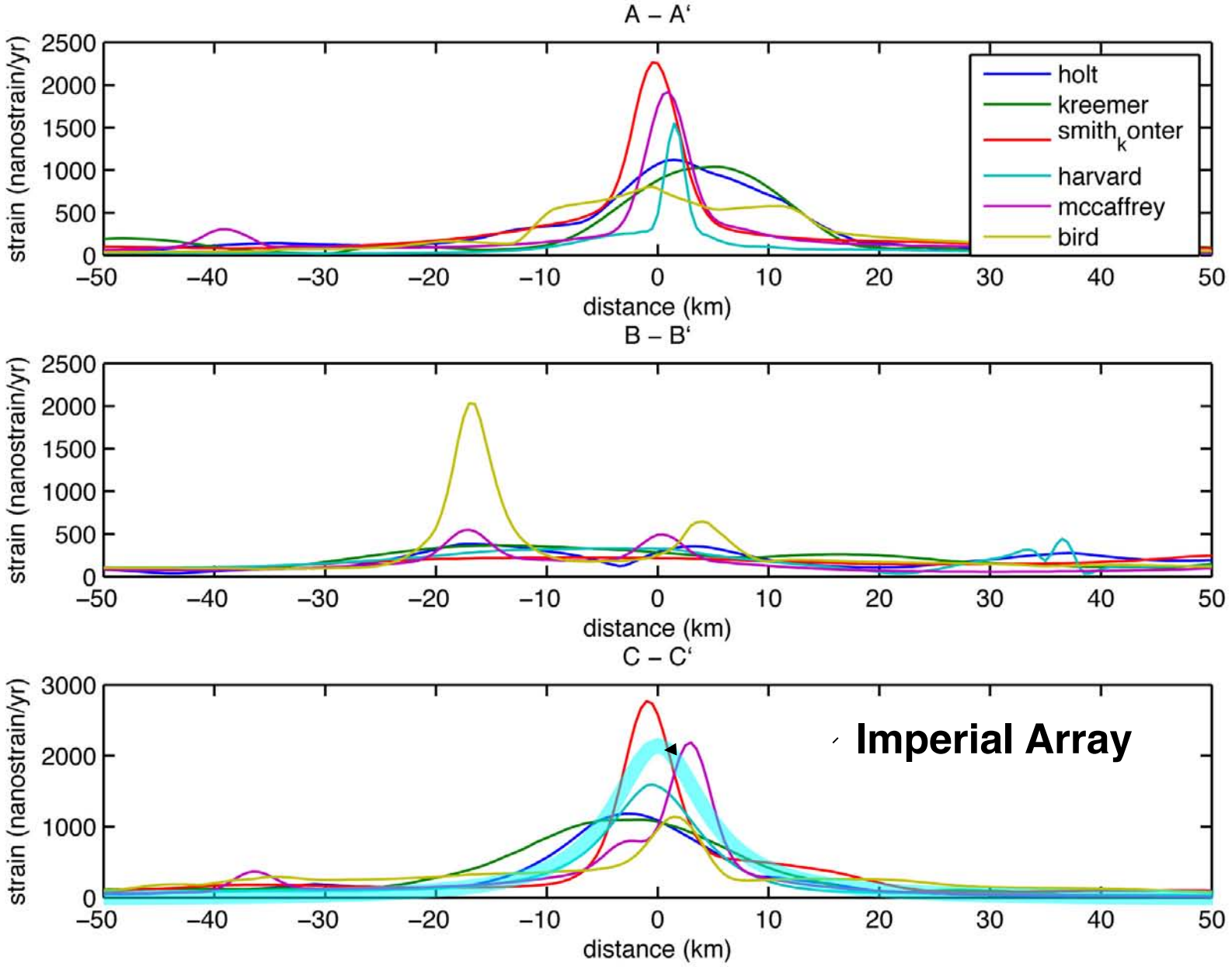

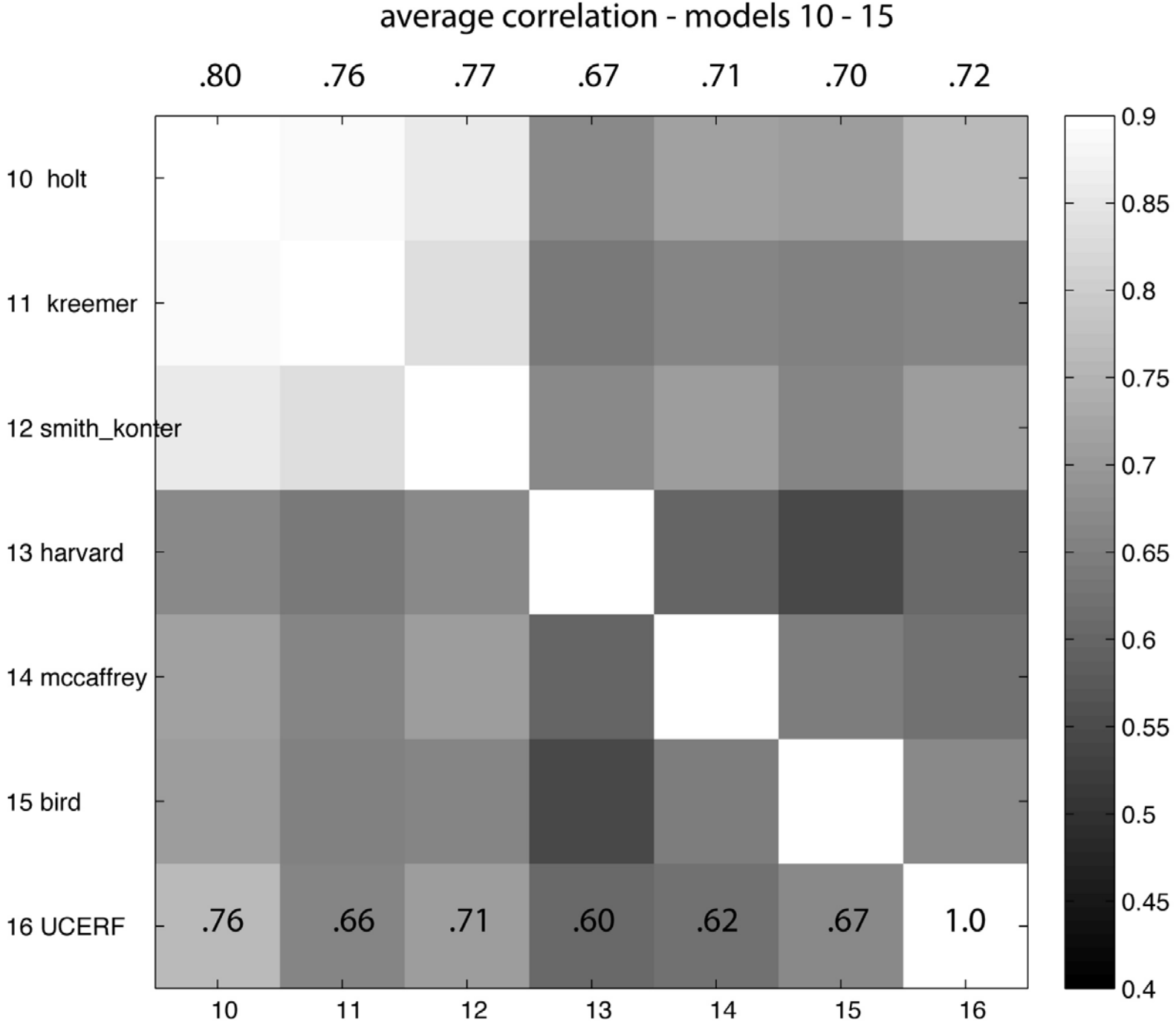
average correlation - models 10 - 15
.80
.76
.77
.67
.71
.70
.72
10 holt
11 kreemer
12 smith_konter
13 harvard
14 mccaffrey
15 bird
16 UCERF
.76
.66
.71
.60
.62
.67
1.0
10
11
12
13
14
15
16
0.9
0.85
0.8
0.75
0.7
0.65
0.6
0.55
0.5
0.45
0.4

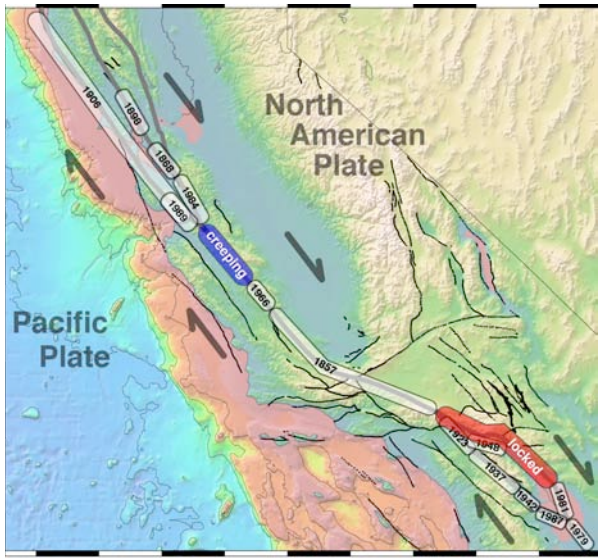

Conclusions

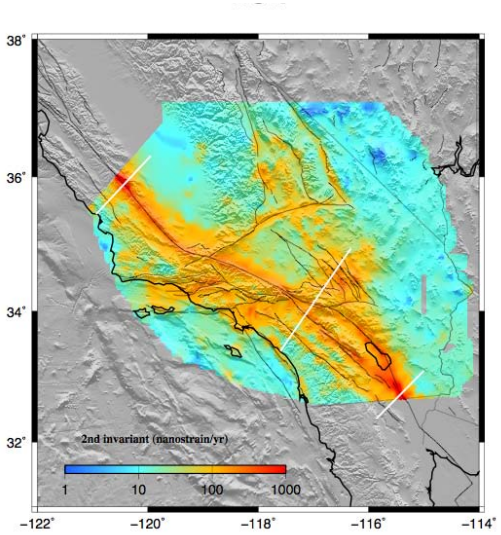

- strain rate = velocity/locking depth; moment rate = velocity X locking depth
- strain rate looks like UCERF2 (best correlation .76)
- strain rate not well resolved by GPS
- block models are best for resolving strain along faults
- how do we decompose strain into elastic and inelastic (e.g. creep)?
- need targeted campaign GPS; need L-band InSAR (e.g. DESDynl

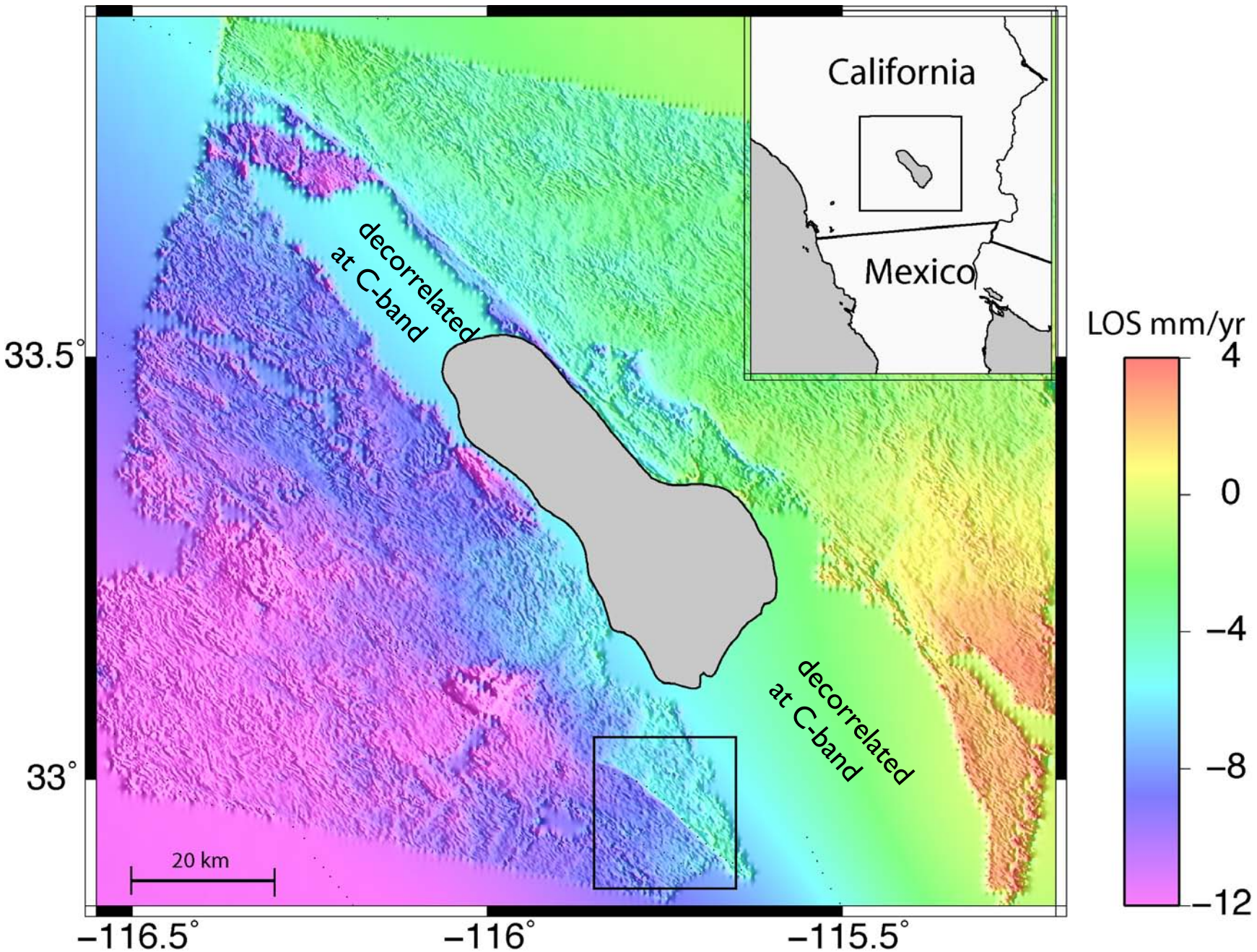
California
Mexico
decorrelated at C-band
decorrelated at C-band
LOS mm/yr
4
0
−4
−8
−12
33.5°
33°
−116.5°
−116°
−115.5°
20 km

Method fails along most of SAF because C-band interferograms are decorrelated.

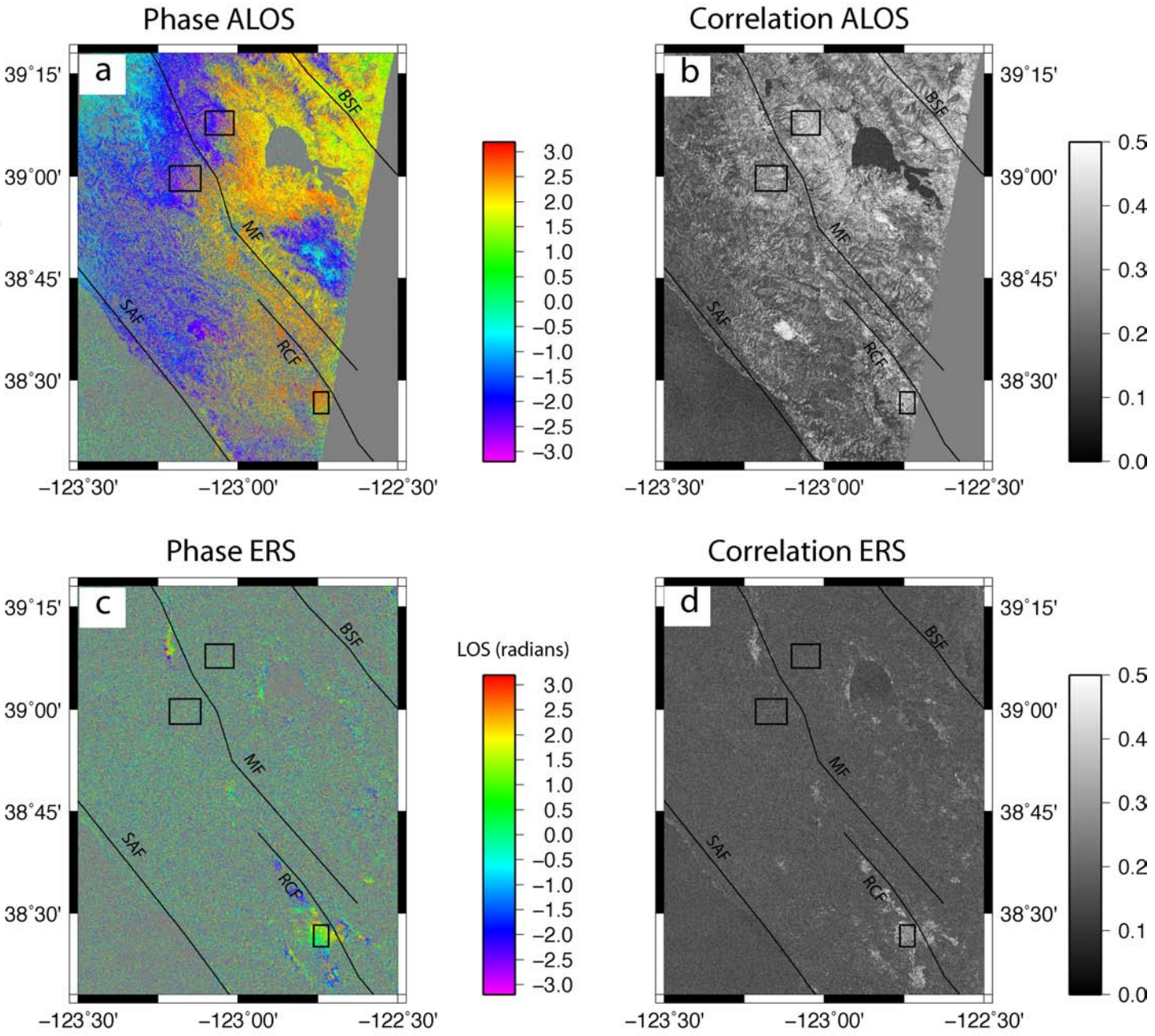

InSAR can also resolve near-fault strain rate

need ~2 mm/yr precision